

ADA 085220

AD

TECHNICAL REPORT  
RPT. NO. TR-80/011

# RETROCKET SOFT LANDING OF AIRDROPPED CARGO

by

William Nykvist

Approved for public release;  
distribution unlimited.

December 1979

UNITED STATES ARMY  
PAK RESEARCH and DEVELOPMENT COMMAND  
WATER, MASSACHUSETTS 01760



Aero-Mechanical Engineering Laboratory

80 6 9 0 60

Approved for public release; distribution unlimited.

Citation of trade names in this report does not constitute an official indorsement or approval of the use of such items.

Destroy this report when no longer needed. Do not return it to the originator.

UNCLASSIFIED

SECURITY CLASSIFICATION OF THIS PAGE (When Data Entered)

14 REPORT DOCUMENTATION PAGE		READ INSTRUCTIONS BEFORE COMPLETING FORM								
1. REPORT NUMBER <b>NATICK/TR-84/011</b>	2. GOVT ACCESSION NO. <b>AD-A085220</b>	3. RECIPIENT'S CATALOG NUMBER <b>9</b>								
4. TITLE (and Subtitle) <b>RETROCKET SOFT LANDING OF AIRDROPPED CARGO</b>		5. TYPE OF REPORT & PERIOD COVERED <b>Technical Report, Oct 1978 - Oct 1979</b>								
7. AUTHOR(s) <b>William E. Nykvist</b>		6. PERFORMING ORG. REPORT NUMBER								
9. PERFORMING ORGANIZATION NAME AND ADDRESS <b>US Army Natick Research and Development Command Aero-Mechanical Engineering Laboratory Natick, MA 01760</b>		10. PROGRAM ELEMENT, PROJECT, TASK AREA & WORK UNIT NUMBERS <b>6.2.1L162210D283 AD 05+</b>								
11. CONTROLLING OFFICE NAME AND ADDRESS <b>US Army Natick Research and Development Command Aero-Mechanical Engineering Laboratory Natick, MA 01760</b>		12. REPORT DATE <b>Dec 1979</b>								
14. MONITORING AGENCY NAME & ADDRESS (if different from Controlling Office)		13. NUMBER OF PAGES <b>1271</b>								
		15. SECURITY CLASS. (of this report) <b>UNCLASSIFIED</b>								
		15a. DECLASSIFICATION/DOWNGRADING SCHEDULE								
16. DISTRIBUTION STATEMENT (of this Report)  <b>Approved for public release; distribution unlimited.</b>										
17. DISTRIBUTION STATEMENT (of the abstract entered in Block 20, if different from Report)										
18. SUPPLEMENTARY NOTES										
19. KEY WORDS (Continue on reverse side if necessary and identify by block number)										
<table border="0"> <tr> <td>PARACHUTE DESCENT</td> <td>RETRO ROCKETS</td> </tr> <tr> <td>CARGO PARACHUTES</td> <td>ROCKETS</td> </tr> <tr> <td>AIR DROP OPERATIONS</td> <td>LANDING IMPACT</td> </tr> <tr> <td>AERIAL DELIVERY</td> <td>SOFT LANDINGS</td> </tr> </table>			PARACHUTE DESCENT	RETRO ROCKETS	CARGO PARACHUTES	ROCKETS	AIR DROP OPERATIONS	LANDING IMPACT	AERIAL DELIVERY	SOFT LANDINGS
PARACHUTE DESCENT	RETRO ROCKETS									
CARGO PARACHUTES	ROCKETS									
AIR DROP OPERATIONS	LANDING IMPACT									
AERIAL DELIVERY	SOFT LANDINGS									
20. ABSTRACT (Continue on reverse side if necessary and identify by block number)										
<p>A retrorocket soft landing system for airdropped cargo is described and mathematically analyzed. Solid propellant rockets and fixed height ground sensing, previously used in the experimental Parachute Retrorocket Airdrop System (PRADS), are assumed for this system. Seventeen variables affecting the load impact velocity are defined and used to write the one-body equations of motion for the system. A computer is used to generate 500 constrained random values for each independent variable, to calculate the impact velocity for 500 cases by solving the equations of motion, and to statistically analyze the results. It is concluded that 95%</p>										

Accession For	
NTIS G-41	<input checked="" type="checkbox"/>
DDC TAB	<input type="checkbox"/>
Unannounced	<input type="checkbox"/>
Justification	<input type="checkbox"/>
By	
Date	
FOR	

DD FORM 1 JAN 73 1473

EDITION OF 1 NOV 65 IS OBSOLETE

UNCLASSIFIED

SECURITY CLASSIFICATION OF THIS PAGE (When Data Entered)

392674

Free

**UNCLASSIFIED**

**SECURITY CLASSIFICATION OF THIS PAGE(When Data Entered)**

20. Abstract (cont'd)

Cont → of the soft landings can be expected to have impact velocities between 2.0 and 3.4 m/s (6.1 and 10.3 ft/s). ↗

**UNCLASSIFIED**

**SECURITY CLASSIFICATION OF THIS PAGE(When Data Entered)**

## PREFACE

The present system of airdropping military cargo and vehicles incorporates paper honeycomb to mitigate impact shock. Paper honeycomb is an effective energy absorber but has several drawbacks which make it difficult to use. The technology of retrorocket deceleration of airdropped loads was advanced considerably in the late 1960's with the development of the Parachute Retrorocket Airdrop System (PRADS). This system used retrorockets to decelerate a rapidly descending airdropped load down to the standard descent rate of about 8 m/s, but relied on paper honeycomb to absorb impact energy. This report investigates the extension of a PRAD-type system to a system where retrorockets provide an actual soft landing, thereby eliminating the need for paper honeycomb.

The author wishes to thank Dr. Edward Ross, NARADCOM Staff Mathematician, for valuable help during the progress of this study.

## TABLE OF CONTENTS

	Page
LIST OF FIGURES	4
LIST OF TABLES	5
INTRODUCTION	7
LITERATURE	8
SYSTEM CHARACTERISTICS	11
DESCRIPTION OF MODEL	18
VARIATION OF INDEPENDENT VARIABLES	24
STATISTICAL ANALYSIS	34
RESULTS AND DISCUSSION	37
CONCLUSIONS	51
REFERENCES	53
APPENDICES:	55
Appendix A. Derivation of Descent Velocity Equation	55
Appendix B. Solution of Equations of Motion for Primary Rocket Deceleration — One-Body Analysis	57
Appendix C. Solution of Equations of Motion for Primary Rocket Deceleration — Two-Body Analysis and Comparison with One-Body Analysis	61
NOMENCLATURE	67

## LIST OF FIGURES

	Page
Figure 1. Load Factor $n$ for Estimating Road Loads	16
Figure 2. Design Condition 1	20
Figure 3. Design Condition 2	21
Figure 4. Interaction of Variables	25
Figure 5. Computer Program Flowchart	36
Figure 6. Percent Change of Descent Velocity, $V_o$ and Rocket Impulses $R_{ptp}$ and $R_{st_s}$ , with Temperature	38
Figure 7. Effect of System Minimum Load Mass on Impact Velocity for $T = 288$ K	41
Figure 8. Frequency Histogram of Variables for System I with $T = 288$ K, Including Skewness (S) and Kurtosis (K) Values	44
Figure 9. Soft Landing System I, 900–25,000 kg	46
Figure 10. Soft Landing System II, 1364–25,000 kg	47
Figure 11. Soft Landing System IV, 2272–25,000 kg	48
Figure 12. Soft Landing System VI, 3180–25,000 kg	49
Figure C1. System Description – Two-Body Analysis	62

## LIST OF TABLES

	Page
Table 1. Summary of Optimum Rocket System for PAD Assisted Parachute System for Aerial Delivery of Cargo	12
Table 2. Summary of Parachute/Retrorocket System for GPADS	13
Table 3. Estimated Maximum Road Loads	17
Table 4. Parachute System	26
Table 5. Variation of Load Mass, M, Four Cases	27
Table 6. Retrorocket Ignition	29
Table 7. Primary Retrorocket Burn Time for RDS-556 Propellant	30
Table 8. Primary Rocket System	32
Table 9. Sustainer Rocket System	33
Table 10. System Minimum Mass	39
Table 11. Impact Time $t_i$	42
Table 12. Comparison of Statistical Parameters for Load Mass (M) and Primary Rocket Thrust/Mass Ratio ( $R_p/M$ )	43
Table 13. Percentage of Impacts Greater than 3.0 and 3.5 m/s	50
Table C1. Comparison of One-Body and Two-Body Analyses for a 8680 kg Load, Three G-12 Parachutes, with $R_p/M = 7G$	66



## RETROCKET SOFT LANDING OF AIRDROPPED CARGO

### INTRODUCTION

The present system of airdropping cargo and vehicles with a mass range of 1800 to 16,000 kg relies on parachutes to achieve a descent velocity of approximately 8 m/s and on paper honeycomb to absorb the impact energy. Although this system is adequate in many respects, several drawbacks have been identified:

- (a) Limitation of 16,000 kg load maximum, with minimum drop altitudes ranging from 335 m to 460 m.
- (b) Lengthy rigging time of the often large, clustered parachutes.
- (c) In large parachute clusters, increased possibility of one or more parachutes failing to inflate.
- (d) Lengthy load preparation time, including need to lift vehicle onto the carefully cut and placed honeycomb before airdrop, and often off it after impact.
- (e) Tendency of loads to overturn in strong surface winds. Paper honeycomb raises the center of gravity and thus increases the tendency to overturn.
- (f) Paper honeycomb bulk a logistic headache — honeycomb has to be stored, shipped, and kept dry. Rigged loads must be protected from rain.

The Parachute Retrorocket Airdrop System (PRADS) used fewer and smaller parachutes to achieve a descent velocity of approximately 16 m/s, used retrorockets to decelerate the load to about 8 m/s at impact, and used paper honeycomb to absorb impact shock. This system improved on drawbacks (a), (b), and (c), above, but can do nothing about drawbacks (d), (e), and (f).

A parachute/soft landing system which achieves a descent velocity much greater than the standard 8 m/s by using fewer small parachutes, and which uses retrorockets to decelerate the load to a velocity near 0 m/s at impact, would improve on all the above-mentioned drawbacks.

There are many ways to perform retrorocket soft landing of airdropped cargo. Possibilities include variable-thrust liquid propellant rockets controlled by an on-board computer, or a microprocessor-controlled thrust deflector system used with solid propellant rockets. Both systems could use a strain gage sensor employed between the parachute and load to accurately "weigh" the load during descent; this information, in conjunction with velocity and altitude data would permit an on-board computer to exactly determine the needed thrust for a perfect soft landing.

As a first look at the problem, however, a less sophisticated retrorocket soft landing system that has several features similar to PRADS will be studied. In this system, the rigged load

weight will determine the number and size of parachutes and solid propellant retrorockets to be used. Fixed height ground sensing is used, which necessitates the use of two retrorocket types — primary and sustainer. Fourteen independent variables which affect the impact velocity are quantitatively and statistically defined. These variables are used in a series of equations which define the load motion. A computer is used to create suitably constrained random values for the variables, to solve the equations of motion and obtain a value of impact velocity in 500 simulated soft landing cases, and to run a statistical analysis of the impact velocity in these 500 cases. In the course of this work approximately 50 of these 500-case statistical analyses were run, covering the ambient temperature range and investigating the effect of many of the variables.

## LITERATURE

In March 1963 a report<sup>1</sup> was published concerning the feasibility of using retrorockets to reduce the descent velocity of an airdropped load from values ranging between 12.2 and 18.4 m/s to an impact velocity of 7.6 m/s. A load range of 900 to 16,000 kg was chosen and was divided into ten classes. In the study a  $\pm 0.9$  m ground sensor error, a  $\pm 1.5$  m rocket ignition ht. variation, and a  $\pm 15\%$  variation in descent velocity were used. It was concluded that high thrust, short burn-time "decelerator rockets" and low thrust, long burn-time "sustainer rockets" could keep impact velocity between 4.8 and 9.0 m/s. A live rocket test was run, with an 1800 kg load dropped from a crane. Ground sensing was successfully carried out with an electronic radar-type ground sensor. The test was not successful due to erratic rocket ignition. The US Army Natick Research and Development Command (then the Quartermaster R&E Command) requested a live rocket airdrop of the propellant actuated device (PAD) assisted parachute system at Yuma Test Station, Yuma Arizona.<sup>2</sup> An 1800 kg load with four G-13 parachutes and six modified M8 rocket motors was airdropped from a 460 m altitude. Five of the six rockets failed to fire, and one rocket fired at impact; the cause for failure was electrical ignition problems. Further testing was suspended pending development of a better rocket retardation system.

In 1965, Stencel Aero Engineering Corp. conducted studies on the Ground Proximity Airdrop System (GPADS) under contract to US Army Natick Research and Development Command (then US Army Natick Laboratories).<sup>3</sup> This exploratory development program

<sup>1</sup> C. J. Litz, Jr. Propellant Actuated Device (PAD) Assisted Parachute System for Aerial Delivery of Cargo. Frankford Arsenal, Philadelphia, PA. Carried out under NARADCOM Project Order QMREC-62-53, March 1963 (AD 415227)

<sup>2</sup> R. A. Neuwen, Jr. An Engineering Evaluation Test of the Rocket Assist Parachute System for Airdrop of Cargo (Phase II — Live Rockets), USATECOM Project No. 4-3-7270-01, YTS Report 3054, Yuma Test Station, Yuma, AZ, August 1963

<sup>3</sup> J. L. Michal. Final Engineering Report — Ground Proximity Airdrop System. Stencel Aero Engineering Corp., US Army Natick R&D Command Technical Report 68-71, September 1966 (AD 837338)

included rocket static testing, hardware design and manufacture, and airdrop tests with and without rocket motors. GPADS was a parachute/retrorocket system having a parachute-decelerated descent velocity between 18.3 and 21.3 m/s, with retrorocket deceleration just prior to impact, resulting in a nominal impact velocity of 7.6 m/s. Limited and successful testing with loads up to 3050 kg from a drop altitude of 91 m, indicated potential performance over a load range of 900 to 16,000 kg. In this system there are 25 weight ranges, three different size parachutes clustered up to 8, and up to 36 rockets required. It was concluded that reliability, weight, bulk, complexity and cost of reusable hardware in GPADS was approximately equal to the present system.

In 1967, the Air Force published a report on a study of aerial delivery of heavy equipment which investigated twelve descent and recovery concepts for the 16,000 to 32,000 kg load range.<sup>4</sup> One of these concepts was the para-rocket system. This system used the extraction parachute as a descent control parachute, with resulting descent velocities between 45 and 53 m/s. A rocket pack with up to eight rocket modules was considered, with each module achieving 120 kN (27,000 lb) thrust for 2.16 s. The ground sensing element would consist of three sounding lines; the longest line would activate the rockets, the next longest line would activate extinction circuits for half the rockets, and the shortest line would activate extinction circuits for the remaining half of the rockets just prior to impact. Rockets would be made "extinct" by means of electrically fired blow-out ports. This was not a soft landing system; normal impact velocity over the entire load range varied from 0.5 to 7.7 m/s, requiring paper honeycomb to absorb impact shock.

Comparison of the para-rocket system to the eleven other concepts concluded:

- (1) Payload recovery from descent velocity to ground impact is best accomplished with a modular rocket package or by disreefing main parachutes.
- (2) Minimum airdrop altitude for the para-rocket system is approximately 213 m as compared to approximately 366 m for an all-parachute system.
- (3) Load tumble in high wind conditions is less frequent in the para-rocket system than with an all-parachute system.
- (4) Cargo landing point scatter is reduced for the para-rocket system in comparison with a low-altitude main disreefing technique for all load extraction altitudes above 366 m.

<sup>4</sup>E. White, C. Bronn, and R. Sturgeon. Study of Heavy Equipment Aerial Delivery and Retrieval Techniques; Lockheed Georgia Co., Contract No. AF33(615)-2989, Air Force Flight Dynamics Laboratory, Wright Patterson AFB, Ohio, AFFDL-TR-66-97, 1967 (AD 810301)

In September 1967 a contract was awarded to Stencel Aero Engineering Corp. for further testing and analysis of the Ground Proximity Airdrop System (GPADS). The GPAD system was previously demonstrated to be feasible in airdrop tests with up to 4550 kg (10,000 lb) loads. For this in-depth exploratory development the name was changed to the Parachute Retrorocket Airdrop System (PRADS). The objectives of the PRADS study were to arrive at a prototype system design and to successfully airdrop a 16,000 kg (35,000 lb) load from 150 m (500 ft) altitude.<sup>5</sup> Several modifications to the GPADS design were made or recommended as a result of the PRADS work. First, the retrorocket motors should be increased in thrust to 57.4 kN (12,900 lb), so that one rocket motor would be needed for approximately 1360 kg of load. For the heaviest load, 16,000 kg, only 12 rocket motors would be required; in the GPAD system 36 rocket motors would have been needed. Secondly, the three parachute sizes of GPADS should be reduced to one, 14.6 m (48 ft) in diameter, clustered up to 8. Third, the ground sensing probes of GPADS should be replaced with a crossed-beam laser ground sensor. One test with such a sensor indicated successful operation. Thirty-four PRADS drop tests were made; 13 drops were with live rockets. A 16,000 kg load was successfully airdropped using eight 14 m diameter parachutes and 32 rockets in tandem rocket packs; the impact velocity was 6.0 m/s. A summary of the PRADS work<sup>6</sup> concluded that a parachute retrorocket recovery system is particularly feasible for the recovery of airdrop loads and may prove to be the only practical system for heavy loads, especially if low altitude is a requirement.

In 1978 a comprehensive study was published of a parachute/retrorocket soft landing system for the B-1 aircraft emergency crew escape module, carried out by the Air Force Flight Dynamics Laboratory.<sup>7</sup> The main system studied consisted of module ejection, descent rate of 12.8 m/s provided by a cluster of three ringsail parachutes, primary retrorocket ignition 2.2 m above the ground with approximately a 0.27 sec delay after burnout, sustainer rocket ignition, impact with vertical velocity less than 3.3 m/s, and sustainer rocket burnout. Included in this voluminous study is an analysis of variations of parameters such as ignition height, descent velocity and impact velocity, a parametric analysis using 5 variables, and detailed design of the retrorockets, pod, and parachutes. Also, an analysis was conducted to determine the optimum descent velocity and thrust/mass ratio, based upon minimum total weight and bulk. It was concluded that, within the boundaries of the somewhat arbitrarily selected landing envelope, the parachute/retrorocket system designed would successfully soft land the escape module.

<sup>5</sup>J. L. Michal, J. L. Oates, and A. L. Martinez. Final Engineering Report, Parachute Retrorocket Airdrop System; Stencel Aero Engineering Corp., US Army Natick R&D Command Technical Report 72-16, December 1970 (AD 736361)

<sup>6</sup>G. Chakoian. A Parachute Retrorocket Recovery System for Airdrop of Heavy Loads; US Army Natick R&D Command Technical Report 70-34-AD, November 1969 (AD 699342)

<sup>7</sup>C. A. Babish et al. A Parachute/Retrorocket Landing System for Aeronautical Vehicles - Study of System Applicability to the B-1 Aircraft Emergency Crew Escape Module; AFFDL-TR-77-140, Air Force Flight Dynamics Laboratory, Wright Patterson AFB, Ohio, February 1978 (AD B031080L)

A Soviet (USSR) parachute/retrorocket system is described in an Army Technical Bulletin on foreign materiel.<sup>8</sup> The system is called the PRS-3500 and was developed in 1965. The system is designed to decelerate loads up to 4000 kg with descent velocities between 18 and 28 m/s, so that an approximate zero impact velocity is achieved. Ground sensing is achieved by two telescopic probes 10 m long, mounted on opposite corners. These probes are adjustable in steps of 10 cm, and telescope on ground contact, after closing the electrical circuit which fires the rockets. The retrorocket unit is a large vertical cylindrical pot fitted with six outwardly canted nozzles at the lower end. The explosive compound used, described by the Soviets as nitroglycerine, is maintained at a certain temperature in the heavily insulated pot. The temperature of the explosive determines its burning rate. Thrust is variable between 166 and 225 kN.

## SYSTEM CHARACTERISTICS

### Details of Previous Retrorocket Systems

Prior to defining the characteristics of the soft landing system to be studied, a closer look at the previous retrorocket airdrop systems will be made. A summary of the optimum rocket system for the Propellant Actuated Device (PAD) Assisted Parachute System (see reference 1) is given in Table 1. This study was based on a primary rocket burn time of 0.2 s and a sustainer rocket burn time of 0.65 s, with average thrust/mass ratios of 8.65 G and 0.87 G, respectively. It was concluded that the ten-class system could decelerate cargo with a load range of 900 to 15,900 kg from a terminal velocity of 15.2 m/s down to 7.6 m/s at ground contact. Terminal descent velocity was assumed to vary  $\pm 15\%$  but no parachute diameters or cluster sizes were given. The means of achieving rocket thrusts listed in the table, i.e., individual rocket thrust values and numbers required, was not given.

A summary of the parachute/retrorocket system of the Ground Proximity Airdrop System (GPADS, reference 3) is given in Table 2. A single rocket size having 18.6 kN (4180 lb) vertical thrust for 0.5 s was used. For the two smallest load classes, parachutes only were used to decelerate the load to the conventional 7 m/s (23 ft/s) impact velocity. Three sizes of parachute were used in GPADS, clustered from three to eight. Two sizes of rocket pack were described: a small pack which could accommodate up to ten rocket motors and a large pack which could accommodate 12 to 18 rocket motors. The average thrust/mass ratio was 4.2 G. The ground sensing probes (two) consisted of mild detonating fuses (MDF) with a firing pin and detonator on the end, wound on a drum prior to deployment. Once the main canopies were deployed, the probes would reel out approximately 8.5 m and would be armed. The descent velocity variation in the table is due to mass variation within a class. Although an air density envelope having air temperatures from 216 to 325 K ( $-70^{\circ}$  to  $+125^{\circ}$ F) and altitudes up to 4100 m (13,500 ft) was given, the effects on descent velocity were not quantified. It was stated that GPADS loads may be dropped when conditions are within the air density envelope, and that conditions outside the envelope may require adjustment of the number of parachutes, number of rockets, or length of the ground sensor probe.

<sup>8</sup>Army Technical Bulletin TB-381-5-11, Foreign Materiel Catalog, Volume II, Aerial Delivery Equipment, Class 1670; Headquarters, Department of the Army, September 1977 (unclassified)

Table 1

Summary of Optimum Rocket System for PAD Assisted Parachute  
System for Aerial Delivery of Cargo (From Reference 1)

Class No.	Mass Range (kg)		Total Thrusts		Thrust/Mass (G)			
	From	To	Decel. (kN)	Sust. (kN)	Decelerator		Sustainer	
					From	To	From	To
I	909	1214	87.6	8.9	9.85	7.38	1.0	0.75
II	1214	1614	117.4	11.9	9.89	7.44	1.0	0.75
III	1614	2150	155.7	15.8	9.86	7.40	1.0	0.75
IV	2150	2864	207.3	21.0	9.85	7.40	1.0	0.75
V	2864	3818	276.7	28.0	9.87	7.40	1.0	0.75
VI	3818	5091	368.3	37.4	9.86	7.39	1.0	0.75
VII	5091	6818	492.4	49.8	9.87	7.37	1.0	0.75
VIII	6818	9091	657.4	66.7	9.85	7.39	1.0	0.75
IX	9091	12045	876.3	89.0	9.85	7.43	1.0	0.75
X	12045	15909	1161.0	117.9	9.85	7.46	1.0	0.76

Table 2

**Summary of Parachute/Retrorocket System for GPADS  
(From Reference 3)**

Mass Range		Parachutes		Descent Velocity		Rockets		Thrust/Mass		Impact Velocity	
From (kg)	To (kg)	No.	DIA (m)	From (m/s)	To (m/s)	No.	Thrust (kN)	Ratio (G) From To		From (m/s)	To (m/s)
909	1364	4	13.7	6.6	8.2	0	0	0	0	6.6	8.2
1364	1695	5	13.7	7.3	8.1	0	0	0	0	7.3	8.1
1695	1909	3	7.3	19.2	20.7	4	74.4	4.5	4.0	6.8	7.7
1909	2000	4	7.3	18.0	18.4	4	74.4	4.0	3.8	7.4	7.7
2000	2409	4	7.3	18.4	20.2	5	93.0	4.7	3.9	7.2	7.7
2409	2500	4	7.3	20.2	20.5	6	111.6	4.7	4.6	6.3	6.4
2500	2909	5	7.3	18.4	19.8	6	111.6	4.6	3.9	7.1	7.7
2909	3045	6	7.3	18.1	18.5	6	111.6	3.9	3.7	7.6	7.9
3045	3636	6	7.3	18.5	20.2	8	148.7	5.0	4.2	7.4	7.1
3636	4000	7	7.3	18.7	19.7	8	148.7	4.2	3.8	7.1	7.9
4000	4818	8	7.3	18.4	20.2	10	185.9	4.7	3.9	7.2	7.7
4818	5455	4	11.0	19.0	20.3	12	223.1	4.7	4.2	6.8	7.1
5455	5909	5	11.0	18.1	18.9	12	223.1	4.2	3.9	7.2	7.7
5909	6818	5	11.0	18.9	20.3	14	260.3	4.5	3.9	6.9	7.8
6818	7727	6	11.0	18.5	19.7	16	297.5	4.5	3.9	7.0	7.6
7727	8636	7	11.0	18.2	19.3	18	334.7	4.4	4.0	7.1	7.5
8636	9545	7	11.0	19.3	20.3	20	371.9	4.4	4.0	6.8	7.6
9545	10455	5	13.7	19.2	20.1	22	409.1	4.4	4.0	6.9	7.5
10455	11364	6	13.7	18.3	19.1	24	466.2	4.4	4.0	7.1	7.4
11364	12273	6	13.7	19.1	19.9	26	483.4	4.3	4.0	6.9	7.4
12273	13182	6	13.7	19.9	20.6	28	520.6	4.3	4.0	6.8	7.5
13182	14091	7	13.7	19.1	19.7	30	557.8	4.3	4.0	6.9	7.3
14091	15000	7	13.7	19.7	20.4	32	595.0	4.3	4.0	6.9	7.4
15000	15909	8	13.7	19.0	19.6	34	632.2	4.3	4.1	6.9	7.3
15909	16818	8	13.7	19.6	20.1	36	669.4	4.3	4.1	6.9	7.3

The Parachute Retrorocket Airdrop System study (PRADS, see references 5 and 6) began with the GPADS configuration outlined in Table 2, and all tests were run with parachutes and rockets as listed therein. There were several recommendations made (see Literature section) regarding parachutes, rockets, and ground sensor. The changes recommended (larger rocket, one-size parachute) would tend to increase variation in descent velocity and thrust/weight ratio; unfortunately, a listing of the proposed PRADS mass ranges and system configuration was not included in references 5 or 6. It was mentioned in reference 5 that retrorockets would be used over the mass range 3600 to 16,000 kg; parachutes only would be used for the 900 to 3600 kg range.

#### Characteristics of the Soft Landing System

All of the aforementioned studies were directed toward achieving an impact velocity of approximately 8 m/s, the value presently used in all-parachute airdrops. A report entitled, "Plan for Advanced Development of a Parachute Retrorocket Airdrop System,"<sup>9</sup> did conclude, however, that PRADS is an extremely versatile concept and later generations of this concept could be used to airdrop all loads with near zero impact velocities so that no energy dissipator would be required. This effort is directed toward achieving just that: elimination of energy dissipator material by using retrorocket deceleration to land the load at low impact velocities.

This initial study of retrocket soft landing examines possibly the least complex method to achieve low impact velocities. The use of fixed-height ground sensing and solid propellant rockets based on the rigged load weight precludes the possibility of a zero-velocity impact under any condition, as will be shown later. The impacts can be kept at a low value, however, and key system variables can be modified to achieve impact velocities below that which causes damage to cargo.

This study is based also on the idea of keeping the system as simple for the user as possible. When the load is rigged for airdrop, experienced riggers will need to consult charts based on load weight to determine the number and size of retrorockets and parachutes. Once the load is rigged, it is final. No corrections are to be made for specific drop conditions as the Soviets do in their system. No retrorockets or parachutes will be added or removed just prior to airdrop to correct for ambient or drop zone conditions. No changes in ground sensor length will be necessary. Indeed, such corrections would greatly increase the possibility of error, would be time consuming, and would be such undesirable changes from the present system, that the entire concept of retrorocket soft landing would be jeopardized. This philosophy will reduce the chance for mistakes.

<sup>9</sup>G. Chakoian. Plan for Advanced Development of a Parachute Retrorocket Airdrop system. US Army Natick Research & Development Command Technical Report 73-59-AD, May 1973 (AD 765422)



In the reference 7 study (retrorocket landing system for B-1 emergency escape module) a detailed analysis was performed to determine the descent velocity and primary rocket thrust/mass ratio (TMR) which would result in minimum total propellant mass. The primary rocket propellant mass was shown to be quite insensitive to increasing TMR, but the sustainer rocket propellant mass was shown to decrease substantially with increasing TMR. The lower primary rocket ignition height and shorter burn time associated with a high value of TMR tend to reduce the magnitude of height error at primary rocket burnout, and therefore greatly reduce sustainer rocket burn time. From a propellant mass standpoint, the TMR should be as large as possible. The effect of descent velocity on the combined mass of the parachute and retrorocket subsystems was also analyzed in reference 7. It was shown that a minimum combined mass existed at a nominal rate of descent of 11.3 m/s. The descent rate selected in reference 7 was 12.8 m/s which resulted in the combined mass being only 3% greater than the minimum. A nominal descent velocity of 16 m/s, in terms of the analysis in reference 7, would represent an increase over the minimum combined parachute and retrorocket mass of 31%. For comparison, the PRAD system employed a nominal descent velocity of 19 m/s and had an average primary rocket TMR of 4.2. Considering all of the above, a value for the primary rocket TMR for this study was chosen to be 7 G, and the nominal descent velocity was chosen to be 16 m/s.

In reference 7, three retrorocket concepts were considered: primary rockets only, primary/sustainer rockets, and primary/delay period/sustainer rockets. Primary rockets are a high thrust, short burn-time type (0.2 to 0.5 second burn) which perform the load deceleration. Sustainer rockets are a low thrust, long burning type (1 to 3 second burn) which reduce the impact velocity in the event the primary rockets burn out with the load some distance above the ground. Sustainer rockets have a thrust equal to about 0.6 to 0.8 times the load weight. In reference 7 the only concept of the three considered feasible was the primary/delay period/sustainer rocket concept. With this in mind, and with the intent of providing the maximum flexibility in the ensuing analysis, the primary/delay period/sustainer rocket concept will be used in this study.

#### Impact Velocity and Load Damage

The impact velocity which just begins to cause vehicular damage will vary for different vehicles. Tracked vehicles are more rugged than soft-wheeled vehicles and can withstand more shock. An AMC Pamphlet, Automotive Bodies and Hulls,<sup>10</sup> gives some idea of the road loads various types of vehicles are capable of withstanding. A road load is defined as a shock initiated at any part of the vehicle which contacts the terrain, and may be in any direction. A semi-empirical procedure in the pamphlet was outlined to determine maximum design loads, and a load factor,  $n$ , was developed. The load factor represents the maximum design acceleration in G's that may be experienced by the front end of the vehicle; failure of some parts at this G level is to be expected. This system of design load estimating was developed for rigid-hulled vehicles such as tanks and armored carriers; the application to wheeled vehicles has been very limited. It is stated that, when applied to trailers or wheeled vehicles, the load factor be used as a general load factor which has a constant value along the length of the vehicle. Figure 1 is reproduced from reference 10. To calculate maximum road loads, the load factor is used in several simple equations, given in Table 3.

<sup>10</sup> Automotive Bodies and Hulls, AMC Pamphlet 706-357, April 1970

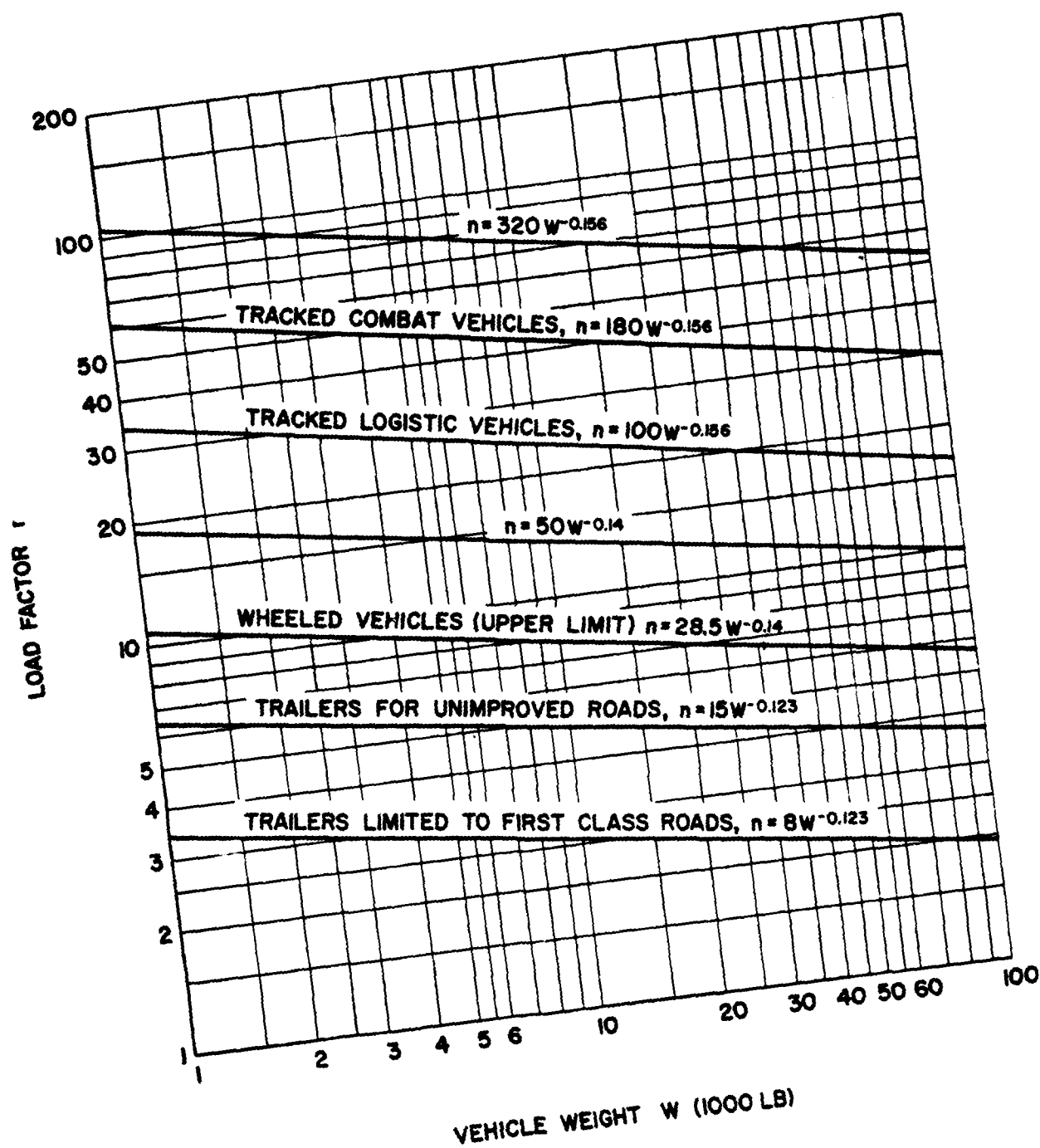


Figure 1. Load Factor  $n$  for Estimating Road Loads

TABLE 3

## Estimated Maximum Road Loads

WHEEL	LOAD EQUATION
Forward sprocket	0.15 nW
No. 1 road wheel	0.10 nW
All other road wheels	0.05 nW
Rear Sprocket	0.07 nW

From this data only maximum wheel forces can be estimated. Figure 1 gives the maximum load factors that different types or classes of vehicles may be subject to. This figure gives a good comparison of the ruggedness of several types of vehicles, but does not provide enough information to determine the safe impact velocity of a given vehicle. Without experimental data it is difficult to relate the G value of an impact to a comparable impact velocity due to the complex dynamic interaction of the vehicle suspension, tires, and terrain.

Dozens of fragility studies were conducted on military vehicles in the 1960's to determine placement and thickness of paper honeycomb beneath the load. There are three reports<sup>11,12,13</sup> which indicate that typical design accelerations of 18 to 20 G were used, resulting in a shock pulse duration of 55–75 ms. In actual drops the average acceleration measured throughout the vehicle was somewhat less than the design acceleration, and the peak acceleration varied from 1½ to 4 times the average acceleration. Acceleration data from these studies, where the load impact velocity was 7.6 to 15.2 m/s, cannot be used to draw conclusions about systems not using paper honeycomb for several reasons. First, the geometrical distribution of input forces is different. The use of paper honeycomb under the engine, transmission, and frame members as well as under the wheels did not permit the normal suspension system of the vehicle to undergo motions that would be achieved in an impact without paper honeycomb. The suspension system of an unprotected (no honeycomb) vehicle would "bottom out" at a relatively low impact velocity. Also, energy absorbed by spring compression would be returned as rebound. Secondly, the relatively slow crush of paper honeycomb reduces the peak

<sup>11</sup>C. Covington and R. Shield. Fragility Studies, Part II, Cargo, Truck, M37, 3/4-Ton; University of Texas Structural Mechanics Research Laboratory, Austin, Texas, April 1960

<sup>12</sup>E. A. Ripperger. Impact Determinations; Final Report, Contract DA19-129-QM-1383, University of Texas Structural Mechanics Research Laboratory, Austin, Texas, 1962 (AD 400638)

<sup>13</sup>E. A. Ripperger. Ground Impact Shock Mitigation; Engineering Mechanics Research Laboratory, University of Texas, Austin, Texas, 1967 (AD 830179)

acceleration but increases the duration of shock input to the vehicle. Once the unprotected vehicle bottoms out the suspension system, the shock pulse will have higher peak acceleration and shorter duration. In a soft landing system, the ruggedness of the specific vehicle suspension system and the terrain characteristics play an important part.

Reference 7 describes a retrorocket soft landing system for the B-1 aircraft emergency crew escape module. The maximum impact acceleration for emergency escape systems is specified in MIL-C-25969 (USAF) in the form of a dynamic response index (DRI) in the vertical direction, and a total acceleration radical.<sup>14</sup> The DRI is representative of the maximum allowable dynamic compression of the human vertebral column. In reference 7, test drops of a full scale escape module indicated that the accelerations were within acceptable MIL-C-25969 limits for a module impact velocity range of 0 to 3.05 m/s (0 to 10 ft/s). Thus the upper limit of impact velocity for the escape module was set at 3.05 m/s. This represents a free fall of only 0.47 m (18.7 in).

Considering military vehicles and cargo, a practical estimate of the maximum soft landing impact velocity can be made by considering free fall heights. It is felt that all military vehicles should at least be able to withstand a 0.30 m (12 in) free fall, equivalent to an impact velocity of 2.4 m/s. A practical estimate of maximum soft landing impact velocity, in terms of reasonable free fall height, is assumed to be between 0.46 and 0.61 m (18 to 24 in). This is equivalent to impact velocity between 3.0 m/s and 3.5 m/s (9.8 to 11.4 ft/s). This is an outright estimate of the maximum allowable impact velocity which does not cause damage to the most fragile of currently airdropped vehicles and cargo.

In summary, a soft landing system will be studied that uses parachutes to decelerate the load to a nominal descent velocity of 16 m/s, uses solid propellant rockets to achieve a nominal primary thrust/mass ratio of 7 G, uses sustainer rockets, after a short delay period, to achieve a nominal thrust/mass ratio of 0.7 G, and uses fixed height ground sensing.

#### DESCRIPTION OF MODEL

In previous work done here at NARADCOM in the soft landing area in 1976-77, a two-body analysis of the parachute/retrorocket/load was used. The parachute was one body, the retrorockets and load the other body. In that analysis the suspension lines and risers were treated as linear springs. The suspension line spring constant had to be calculated, and the length and number of lines were needed to calculate the relative positions of the two bodies under various system conditions. In Appendix C, an outline of the two-body analysis is given, along with a specific example of a 8680 kg load using three G-12 (19.5 m diameter) parachutes. For comparison, a one-body analysis, identical to that used throughout this report, was carried out on the same example case. The differences in the altitude and velocity during primary rocket burn are very slight. The one-body analysis facilitates the problem by allowing an exact solution to the differential equations of motion, without introducing significant error.

<sup>14</sup> Military Specification MIL-C-25969 (USAF), Capsule Emergency Escape Systems, General Requirements for, 4 March 1970

In developing the model, several assumptions were made concerning conditions during the last few seconds of an airdrop. It is assumed the load may be swinging under the parachute and that the angle from the vertical,  $\theta$ , varies between  $-10^\circ$  and  $+10^\circ$ . It is assumed the terrain may be sloping, and that the slope of the terrain,  $\alpha$ , varies between  $-5^\circ$  and  $+5^\circ$  from the horizontal. The load may have a horizontal velocity, due to winds or load oscillation of 0 to 10 m/s just prior to impact.

There are two extreme conditions possible in any airdrop. Design condition 1 is the extreme case where the descent velocity is at a maximum, the thrust at a minimum, the load tipped so the probe (or ground sensor) is at the maximum angle from the vertical, and the horizontal velocity is at a maximum with the system traveling at the maximum upslope. This is illustrated in Figure 2. The opposite situation, design condition 2, is illustrated in Figure 3. In these two figures the load is pictured at probe contact along with the trajectory it would follow under the design condition. These trajectories are divided into regions represented by Roman numerals. Here a rigid probe is shown as the ground sensor. If a laser ground sensor is used, the mounting would be on the load platform and the laser beams would be affected by load swinging just as a rigid probe would.

The equations for each of the regions are as follows:

**REGION I – Sensor delay and thrust buildup**

$$H_0 = L(\cos\theta + \sin\theta \tan\alpha) \quad (1)$$

$H_0$  = height above ground at probe contact, m

$L$  = probe length, m

$\theta$  = load attitude angle, deg (+ is to right of vertical)

$\alpha$  = terrain slope, deg (+ is uphill)

$$H_1 = H_0 - V_0 t_r - V_h t_r \tan\alpha \quad (2)$$

$H_1$  = height at start of primary rocket thrust, m

$t_r$  = sensor delay and thrust buildup time, s

$V_0$  = initial vertical descent velocity, m/s (+ is downward)

$V_h$  = horizontal velocity, m/s

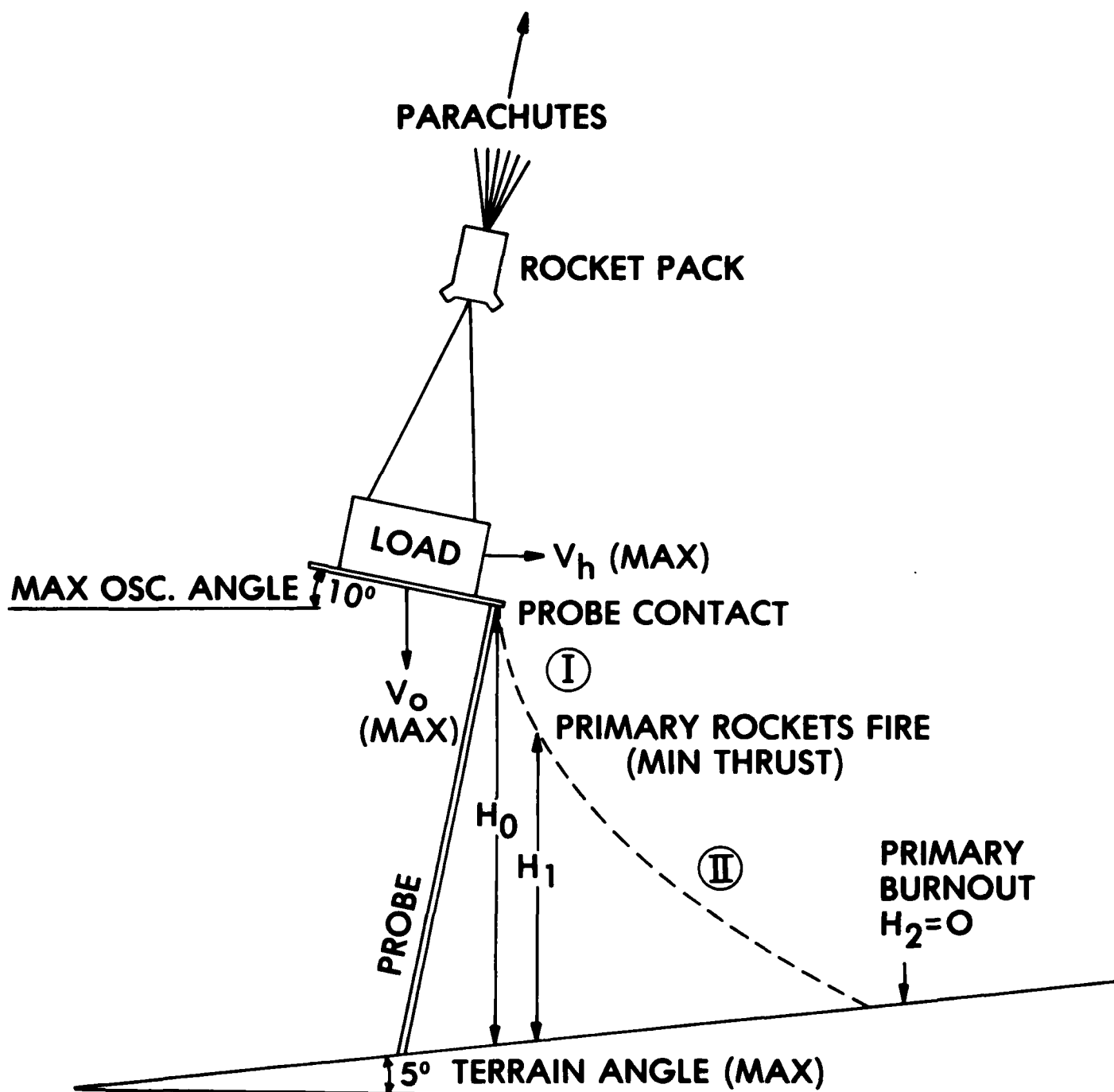


Figure 2. Design Condition 1

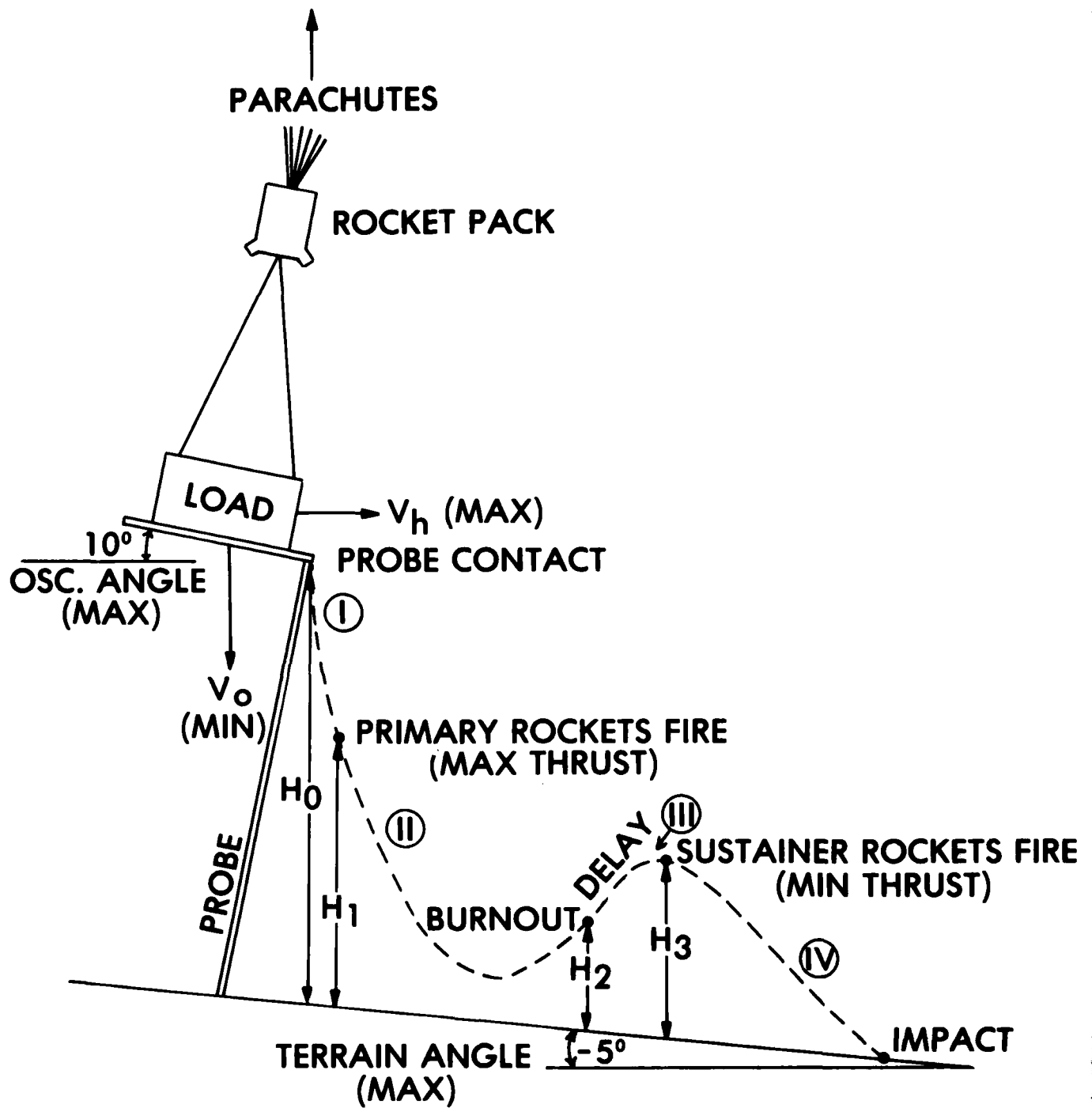


Figure 3. Design Condition 2

$$V_o = \left[ \frac{0.574 MGT}{P_o (NFC_{DS}) A_f} \right]^{1/2} \quad (3)$$

$$\text{where } A_f = \left( 1 - \frac{A}{44334} \right) 5.2561 \quad (4)$$

M = system mass, kg

G = gravitational constant = 9.8 m/s<sup>2</sup>

T = air temperature at drop zone, K

P<sub>o</sub> = sea level pressure, kPa

N = number of parachutes

F = cluster factor

C<sub>D</sub> = drag coefficient of parachute

S = nominal parachute area, m<sup>2</sup>

A = altitude above sea level, m

A<sub>f</sub> = altitude factor

The sign convention for velocity is plus represents downward. For derivation of equations (3) and (4) see Appendix A.

#### REGION II – Primary rocket deceleration

$$V_2 = \frac{a}{\sqrt{ab}} \tan \left[ \sqrt{ab} (t_p + c) \right] \quad (5)$$

$$H_2 = H_1 + \frac{1}{b} \ln \left[ \cos(\sqrt{ab} (t_p + c)) \right] - \frac{1}{b} \ln \left[ \cos(c \sqrt{ab}) \right] - V_h t_p \tan \alpha \quad (6)$$

$$\text{where } a = G - \frac{R_p}{M} \quad (7)$$

$$b = - \frac{G}{V_o^2} \quad (8)$$

$$c = \frac{\tan^{-1} \left[ \frac{V_o \sqrt{ab}}{a} \right]}{\sqrt{ab}} \quad (9)$$

t<sub>p</sub> = primary rocket burn time, s



$R_p$  = total primary rocket thrust, N

$V_2$  = load vertical velocity at end of burn, m/s

$H_2$  = load height at end of burn, m

$$\text{Also, } R_p = R_{pn} \left[ 1 + 0.00198 (T_p - 288) \right] \quad (10)$$

where  $R_{pn}$  = nominal primary rocket thrust

at  $T_p = 288$  K

$T_p$  = propellant temperature, K

For derivation of equations (5) and (6) see Appendix B. Equation (10) is from reference 7.

### REGION III -- Delay period

$$V_3 = V_2 + Gt_d \quad (11)$$

$$H_3 = H_2 - V_2 t_d - \frac{Gt_d^2}{2} - V_h t_d \tan \alpha \quad (12)$$

where  $t_d$  = delay time, s

$V_3$  = vertical velocity at end of delay period, m/s

$H_3$  = height at end of delay period, m

### REGION IV -- Sustainer rocket deceleration

$$V_i = \left[ G - \frac{R_s}{M} \right] t_i + V_3 \quad (13)$$

$$t_i = \frac{(-V_3 + V_h \tan \alpha) + \sqrt{(-V_3 + V_h \tan \alpha)^2 + 2H_3 (G - R_s/M)}}{(G - R_s/M)} \quad (14)$$

$$R_s = R_{sn} \left[ 1 + 0.00198 (T_p - 288) \right] \quad (15)$$

where  $V_i$  = vertical impact velocity, m/s

$t_i$  = time from sustainer start to impact, s

$R_s$  = sustainer rocket thrust, N

$R_{sn}$  = sustainer rocket thrust at  $T_p = 288$  K, N

## VARIATION OF INDEPENDENT VARIABLES

The relationships among the variables for the equations developed in the previous section have been charted in Figure 4. From this figure it is seen that drop zone ambient temperature  $T$  affects  $T_p$  and  $V_o$ , and  $T_p$  in turn affects all rocket thrusts. The dotted lines between  $A$ ,  $T$ , and  $T_p$  imply that altitude affects ambient temperature to some degree, and that propellant temperature  $T_p$  is affected by  $T$ . For the purposes of this study,  $T$  will be assumed independent of  $A$ , and  $T_p$  will be assumed to be the same as  $T$ . Since temperature  $T$  affects several variables, it must be factored out to keep the variables independent. This is done herein for  $t_p$ ,  $R_p/M$ ,  $R_s/M$  and  $t_s$ , by assuming nominal values occur at  $T = 288$  K, and having a temperature correction for any other values of  $T$ . In any ambient temperature other than 288 K, the mean value of the independent variables will change but the standard deviation remains unchanged.

In this section the independent variables  $M$ ,  $P_o$ ,  $NFC_{DS}$ ,  $A_f$ ,  $V_h$ ,  $\alpha$ ,  $\theta$ ,  $t_p$ ,  $L$ ,  $t_r$ ,  $R_p/M$ ,  $R_s/M$ ,  $t_s$  and  $t_d$  will be quantitatively defined with a mean value and a standard deviation. For variables which are assumed to have a normal distribution, the standard deviation will be found by dividing the estimated maximum deviation from the mean by 3.5. In other words, the maximum value is assumed to be 3.5 standard deviations from the mean. In a normal distribution the probability that a random variable is within  $\pm 3.5 \sigma$  of the mean is 99.95%.

### (a) Load Mass, $M$

The variation of  $M$  depends entirely upon the choice of a parachute system. The parachute system proposed for this soft landing study is designed to minimize variation in descent velocity. A standard atmosphere (nominal) descent velocity of 16 m/s was chosen, which is approximately double that of the currently used all-parachute system. For comparison, PRADS used a nominal descent velocity range of 16.7 to 21.3 m/s, and reference 7 used a value of 12.8 m/s. Table 4 summarizes the parachute system used in this study.

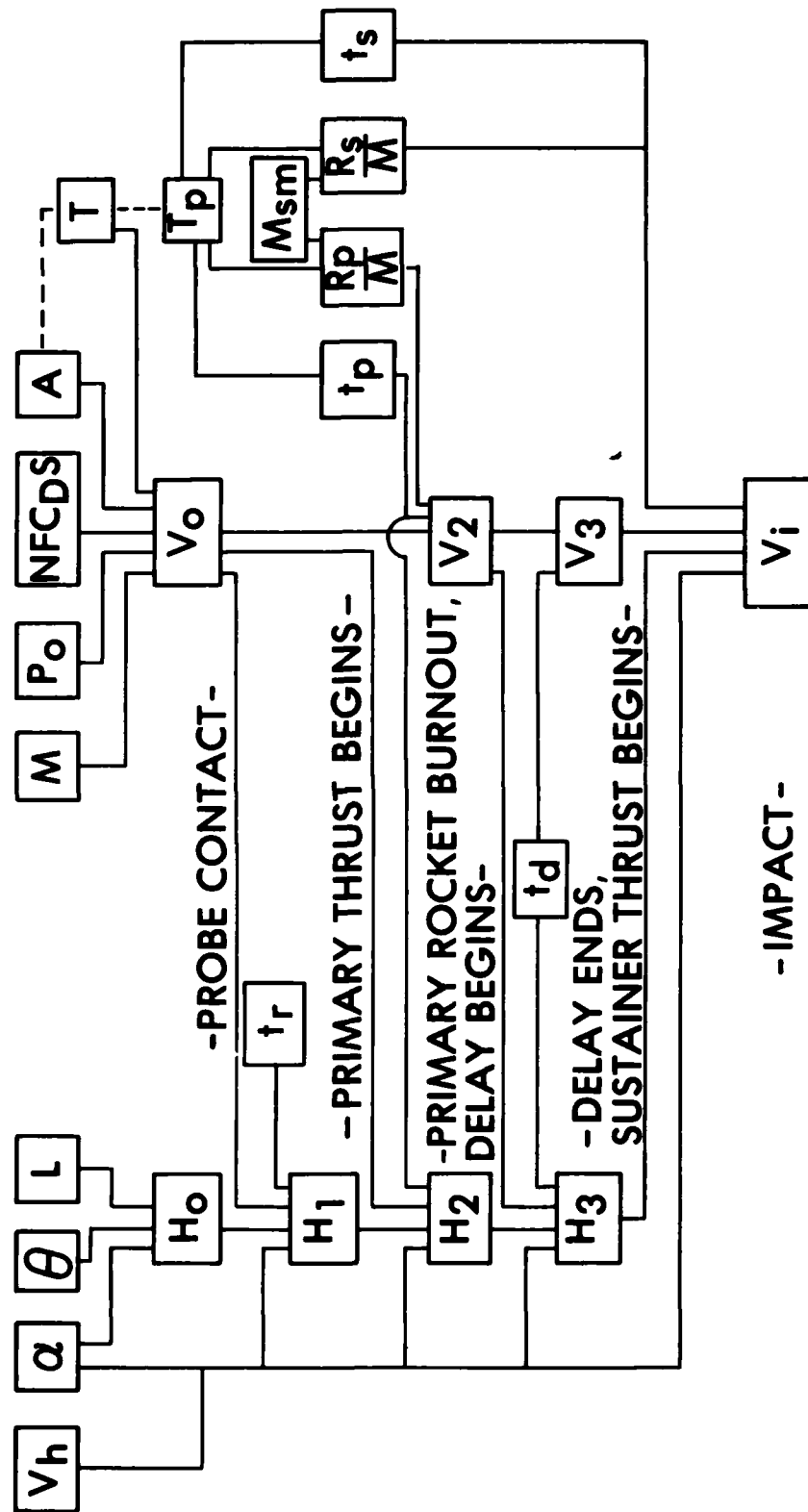


Figure 4. Interaction of Variables

TABLE 4

## Parachute System

Load Mass Range (kg)		Parachutes		Descent Velocity in Standard Atmosphere (m/s)	
From	To	Number	Diameter (m)	From	To
900	1150	3	6.5	15.0	17.0
1150	1440	4		15.0	16.7
1440	1700	5		15.2	17.0
1700	2070	6		15.4	17.0
2070	2650	3	9.8	15.0	17.0
2650	3300	4		15.0	16.7
3300	3910	5		15.2	16.5
3910	4760	6		15.4	17.0
4760	6100	3	14.9	15.0	17.0
6100	7600	4		15.0	16.7
7600	9000	5		15.2	16.6
9000	10950	6		15.4	17.0
10950	14000	3	22.6	15.0	17.0
14000	17500	4		15.0	16.7
17500	20700	5		15.2	16.6
20700	25000	6		15.4	16.9

To achieve the minimum variation about the descent velocity of 16 m/s, as well as to extend the airdrop load mass to 25,000 kg (55,000 lb), four parachute sizes were needed, clustered from 3 to 6. Equation (3) was used to calculate descent velocity using standard sea-level values for  $T$ ,  $P_0$  and  $A_f$ .

Since the mass of an airdropped load may fall randomly within a load range, it is assumed the distribution of  $M$  is uniform.

According to R. L. Wine,<sup>15</sup> for a uniformly distributed variable over the range (d, e), the mean, m, and standard deviation,  $\sigma$ , are

$$m = \frac{d + e}{2} \quad \text{and} \quad \sigma = \left[ \frac{(e - d)^2}{12} \right]^{1/2} \quad (16)$$

From this relation it is seen that  $\sigma$  will differ for each mass range. Four example mass ranges from Table 4 are examined in Table 5.

TABLE 5  
Variation of Load Mass, M, Four Cases

Mass Range (kg)		Mean (kg)	$\sigma_m$ (kg)	$\frac{\sigma_m}{\text{Mean}}$
From	To			
900	1150	1025	72.2	0.070
2650	3300	2975	187.6	0.063
7600	9000	8300	404.1	0.049
20700	25000	22850	1241.3	0.054

The average value of  $\sigma_M/\text{mean}$  for all 16 mass ranges is 0.060; for the statistical analysis the approximately average case of  $M = 2975$  kg and  $\sigma_M = 187.6$  kg will be used.

(b) Sea Level Pressure,  $P_0$

From the Handbook of Geophysical & Space Environments,<sup>16</sup> the sea level pressure between latitudes 10°N to 80°N and longitudes 70°W to 20°E is normally distributed with a mean value of 101.33 kPa and a standard deviation of 0.67 kPa.

(c) Drag Area,  $NFC_D S$

In reference 7 a statistical analysis was made of a large amount of data from drop tests of single and clustered Ringsail-type parachutes to determine the variation in descent system drag area to produce the observed variation in rate of descent. Factors affecting the descent velocity were vertical wind velocities, system oscillations, parachute construction, rigging, and descent shape. For a Ringsail-type parachute,  $\sigma/\text{mean}$  for the rate of descent due to variations

<sup>15</sup> R. L. Wine. Statistics for Scientists and Engineers; Prentice-Hall, Englewood Cliffs, NJ, 1964

<sup>16</sup> Handbook of Geophysical & Space Environments, Air Force Cambridge Research Laboratory, USAF, 1965

in influencing parameters other than system weight and air density was calculated to be 0.042. Although this was calculated for Ringsail parachutes, it is assumed that it is a good estimate for any parachute.

For the example case of  $M = 2975$  kg, the requirement of four 9.8 m diameter parachutes is determined from Table 4. The drag area,  $S$ , for one parachute is  $75.43 \text{ m}^2$ . From AMC Pamphlet 706-130<sup>17</sup> the value of  $F$ , the cluster factor, for four parachutes is 0.825, and the drag coefficient  $C_D$  is typically 0.75. Then the mean value of  $NFC_DS$  is  $186.7 \text{ m}^2$  and  $\sigma NFC_DS$  is  $7.8 \text{ m}^2$ .

(d) Altitude Factor,  $A_f$

Equation (4) indicates that  $A_f$  depends on  $A$ , the altitude above sea level. It is assumed that  $A$  can range from 0 to 1525 m (5000 ft), giving a range for  $A_f$  from 1 to 0.832. Since  $A$  can vary randomly over the entire range, it is assumed to have a uniform distribution. Using equation (16), the mean value of  $A_f$  is 0.916 and  $\sigma_{A_f}$  is 0.049.

(e) Horizontal Velocity,  $V_h$

The system horizontal velocity is assumed to have a maximum of 10 m/s. It is assumed to be uniformly distributed, and from equation (16) the mean value of  $V_h$  is 5 m/s and  $\sigma_{V_h}$  is 2.9 m/s.

(f) Terrain Slope,  $\alpha$

For this study, a terrain slope variation of  $\pm 5^\circ$  is assumed. A normal distribution of  $\alpha$  is assumed with mean value of 0.0. The maximum variation of  $5^\circ$  is assumed to be 3.5 standard deviations from the mean, so  $\sigma_\alpha$  is  $1.43^\circ$ .

(g) System Oscillation Angle,  $\theta$

It is assumed that system oscillations during parachute descent will vary as  $-10^\circ \leq \theta \leq 10^\circ$ . Assuming a normal distribution, the mean value of  $\theta$  is 0.0 and  $\sigma_\theta$  is  $2.86^\circ$ .

(h) Probe Length,  $L$

The variation in probe length depends upon the type of probe or ground sensing device used. In reference 7, a rigid, telescoping probe with a mechanical limiter was used to achieve a variation in  $L$  of only  $\pm 6.4$  mm. The PRAD system used a crossed-beam laser ground sensing device which had a variation of  $\pm 0.30$  m for a 0.15 m lens separation, but could achieve  $\pm 0.15$  m with a lens separation of 0.38 m. It should be noted that the value of  $L$  used in reference 7 was 2.7 m, while that for the PRAD system was 7.6 m.

<sup>17</sup> Engineering Design Handbook, Design for Air Transport and Airdrop of Materiel, AMC Pamphlet 706-130, Hq, US Army Materiel Command, December 1967

For this study, the variation of  $L$  will be assumed to be  $\pm 0.1$  m. At the beginning of this study  $L$  was an unknown quantity; it was set at 3.42 m by the criterion of not having load impact before primary rocket burnout at design condition 1. The standard deviation of  $L$  is 0.029 m.

(i) Sensor Delay and Thrust Buildup Time,  $t_r$

In reference 7 the retrorocket ignition system was characterized by three events, with the following time breakdown:

TABLE 6

Retrorocket Ignition

Event	Mean Time (s)	Percent of Total Time
1. Probe contact to start of shielded mild detonating cord (SMDC) burn	0.0015	3.9
2. SMDC burn time, probe to ignitor	0.0023	5.9
3. Start of ignitor to start of thrust buildup	<u>0.035</u>	<u>90.2</u>
TOTALS	0.039	100.0

Over 90% of the total time is due to the start of the ignitor and thrust buildup. Although a SMDC will probably not be used in a cargo retrorocket system, the total ignition time of 0.039 s, with a standard deviation of 0.003 s is used in this study. It is good approximation due to the dominance of the ignitor start and thrust buildup time, which is independent of the means of transferring the probe sensor signal to the ignitor.

(j) Primary Rocket Burn Time,  $t_p$

According to F. A. Warren,<sup>18</sup> the burning rate of a solid propellant is inversely proportional to  $(T_o - T_p)$  where  $T_o$  is constant characteristic temperature based upon the specific propellant, typically about 470 K. Then as  $T_p$  increases,  $(T_o - T_p)$  decreases, and burning rate increases. This is borne out by data in reference 7 for RDS-556 propellant used in the primary retrorockets. Burning rate and time for various temperatures is shown in Table 7.

<sup>18</sup>F. A. Warren. Rocket Propellants; Reinhold Pub. Corp., New York, 1958

TABLE 7

**Primary Retrorocket Burn Time for RDS-556  
Propellant (from Reference 7)**

Temperature, K	219	233	288	322	366
Burning rate at 2000 psi, (in/s)	1.9	1.94*	2.09*	2.18*	2.3
Burn time for 1 in (s)	0.53	0.52	0.48	0.46	0.43
Percent change from burn time at T = 288 K	+9.1	+7.7	0	-4.1	-9.1

\*Linearly interpolated values

From this table the following equation for primary burn time is written:

$$t_p = t_{pn} [1 - 0.0013 (T_p - 288)] \quad (17)$$

where  $t_{pn}$  is the burn time at the nominal propellant temperature of 288 K.

The value of  $t_{pn}$  also varies due to slight differences in propellant composition, combustion, and weight among individual retrorockets. From the report of J. F. Clark, Jr.,<sup>19</sup> the PRADS retrorocket motors were designed to have a burn time of  $0.46 \pm 0.030$  seconds at standard conditions. This is equivalent to a burn time of  $0.460 \text{ s} \pm 6.5\%$ . We assume a normal distribution, so that  $\sigma_{t_{pn}}$  is  $0.018 t_{pn}$ .

(k) Primary Rocket Thrust/Mass,  $R_p/M$

Equation (10) shows  $R_p$  to be a function of  $T_p$  and  $R_{pn}$ . For a given value of  $T_p$ , the variation of  $R_p/M$  is entirely dependent upon the choice of a retrorocket system.

In the system under study, the nominal primary thrust/mass ratio  $R_p/M$  was chosen to be 7 G. A proposed primary rocket system is described in Table 8. Because discrete numbers of rocket motors with specific thrusts are used, the value of  $R_p/M$  will vary within a mass range, and will equal the chosen value of 7 G only at the center of the mass range. As the load mass increases from top to bottom in Table 8, the ratio of the minimum thrust increment to the average mass decreases. This fact was used in constructing Table 8. At the lower load masses the thrust increment is 20 kN; at the intermediate load masses it is

<sup>19</sup>J. F. Clark, Jr., Development of Rocket Motor for Parachute Retrorocket Airdrop System, Frankford Arsenal, Philadelphia, PA, June 1973



50 kN; and at the higher load mass it is 100 kN. This primary rocket system requires a maximum of 12 rockets, and up to a 16,000 kg load requires only 3 rocket sizes. Between a 16,000 and 25,000 kg load mass one more rocket size (200 kN thrust) is necessary to keep the total number of rockets 12 or less. The 12-rocket cluster size allows a balanced addition of 2, 3, 4, 6, 8, 10 or 12 rockets; this balance is necessary to keep the thrust vector aligned with the axis of the parachutes and load. There is only one case in each of Tables 8 and 9 where perfect thrust balance is not achieved; these cases involve using 5 rockets, which cause only a minimum imbalance.

For the mass range of 900 kg to 25,000 kg the variation of  $R_p/M$  is from 6.00 to 7.99 G, with mean value of 7 G. Although the distribution of  $R_p/M$  within a mass range is expected to be uniform, the variation of the extreme values of  $R_p/M$  from the lightest masses to the heaviest is justification to assume  $R_p/M$  to be normally distributed. The standard deviation of  $R_p/M$  is 0.29 G.

#### (l) Sustainer Rocket Thrust/Mass, $R_s/M$

Sustainer rockets are necessary to reduce the pull of gravity in the likely event that primary rocket burnout occurs with the load some distance above the ground. For example, a free fall of 1 m from zero velocity would result in an impact velocity of 4.4 m/s. Adding retrorockets with a value of  $R_s/M$  of 0.7 G would reduce the impact velocity in the above example to 2.4 m/s. Although the impact velocity is only approximately halved, the kinetic energy, which is based on the square of the velocity, is reduced by a factor of almost 4. During the course of this study it was found that a value of  $R_s/M$  of 0.7 G gave the best results. Values less than 0.7 G did not provide enough thrust to adequately slow descent, and greater values excessively increased sustainer burn time.

A proposed sustainer rocket system is shown in Table 9. Two rocket sizes, 3.6 kN and 20 kN, were used to cover the entire load mass range; a maximum of 12 rockets is needed. If three rocket sizes were used instead, probably a smaller number of rockets would be needed for a given load mass. It is felt that fewer sizes of rockets is important from the logistics and complexity viewpoint. This table was constructed in the same way as Table 8, with corresponding similarities. The variation of  $R_s/M$  is largest for the small load masses and smallest for the large load masses. The variation in  $R_s/M$  for the 900 to 25,000 kg system is 0.56 G to 0.84 G. The mean value of  $R_s/M$  is 0.7 G, with standard deviation 0.04 G. If the minimum load mass were increased to 1364 kg, the variation in  $R_s/M$  would be 0.60 G to 0.81 G, a reduction of 23%.

#### (m) Sustainer Rocket Burn Time, $t_s$

Since the sustainer rocket total thrust will not exceed the load weight, all that is required is that  $t_s$  be long enough so that burnout is after touchdown for all cases. Although the propellant for the sustainer rockets will be different than that in the primary rockets, it is assumed that the burn time/temperature relation is approximately the same. In accordance with equation (17)

$$t_s = t_{sn} (1 - 0.0013(T_p - 288)) \quad (18)$$

Table 8

## Primary Rocket System

Thrust, $R_p$ (kN)	Mass Range (kg)		Thrust/Mass Ratio, $R_p/M$ (G)		Number Of Rockets With Thrust Of :			
	From	To	From	To	10kN	50kN	100kN	200kN
60	900	1021	6.80	6.00	6			
80	1021	1312	7.99	6.22	8			
100	1312	1603	7.78	6.37		2		
120	1603	1895	7.64	6.46	2	2		
140	1895	2187	7.53	6.53	4	2		
160	2187	2477	7.46	6.59	6	2		
180	2477	2769	7.41	6.63	8	2		
200	2769	3061	7.37	6.67			2	
220	3061	3353	7.33	6.70	2		2	
240	3353	3644	7.30	6.72	4		2	
260	3644	3935	7.28	6.74	6		2	
280	3935	4227	7.26	6.76	8		2	
300	4227	4738	7.24	6.46		2	2	
350	4738	5467	7.54	6.53		3	2	
400	5467	6196	7.47	6.59			4	
450	6196	6925	7.41	6.63		3	3	
500	6925	7653	7.37	6.67		2	4	
550	7653	8381	7.33	6.70		3	4	
600	8381	9110	7.31	6.72			6	
650	9110	9840	7.28	6.74		3	5	
700	9840	10933	7.26	6.53		2	6	
800	10933	12390	7.46	6.59			8	
900	12390	13848	7.41	6.63		2	8	
1000	13848	15306	7.37	6.67			10	
1100	15306	16764	7.33	6.69		2	10	
1200	16764	18222	7.30	6.72				6
1300	18222	19679	7.28	6.74		2		6
1400	19679	21137	7.26	6.76			2	6
1500	21137	22595	7.24	6.77			3	6
1600	22595	24052	7.23	6.79				8
1700	24052	25510	7.21	6.80		2		8

Table 9

## Sustainer Rocket System

Thrust, $R_s$ (kN)	Mass Range (kg)		Thrust/Mass Ratio, $R_s/M$ (G)		Number Of Rockets With Thrust Of	
	From	To	From	To	3.6kN	20kN
7.2	900	1312	0.82	0.56	2	
10.8	1312	1837	0.84	0.60	3	
14.4	1837	2362	0.80	0.62	4	
18.0	2362	2887	0.78	0.64	5	
21.6	2887	3433	0.76	0.64	6	
25.2	3433	3958	0.75	0.65	7	
28.8	3958	4461	0.74	0.66	8	
32.4	4461	4986	0.74	0.66	9	
36.0	4986	5540	0.74	0.66	10	
40.0	5540	6356	0.74	0.64		2
47.2	6356	7405	0.76	0.65	2	2
54.4	7405	8455	0.75	0.66	4	2
61.6	8455	9505	0.74	0.66	6	2
68.8	9505	10845	0.74	0.65	8	2
80.0	10845	12187	0.75	0.67		4
87.2	12187	13236	0.73	0.67	2	4
94.4	13236	14285	0.73	0.67	4	4
101.6	14285	15335	0.73	0.68	6	4
108.8	15335	16677	0.72	0.67	8	4
120.0	16677	18018	0.73	0.68		6
127.2	18018	19067	0.72	0.68	2	6
134.4	19067	20116	0.72	0.68	4	6
141.6	20116	21982	0.72	0.66	6	6
160.0	21982	23849	0.74	0.68		8
167.2	23849	24898	0.72	0.69	2	8

A variation in  $t_{sn}$  of  $\pm 6.5\%$ , similar to that of  $t_{pn}$ , is also assumed. Then  $\sigma_{t_{sn}} = 0.018 t_{sn}$ .

(n) Delay Time,  $t_d$

The delay time is needed to allow the upward velocity of the load to quickly drop to near zero when conditions are such that an upward velocity exists. If there were no delay, sustainer rockets would have to burn considerably longer, adding needless extra weight to the system.

At probe contact, a sustainer rocket delay relay would be energized. This relay would delay sustainer rocket ignition until 0.15 s after primary rocket burnout. This 0.15 s time was found by trial and error; it is the time which gave the overall lowest impact velocity.

Since the relay must be initiated at probe contact, the actual time delay is the difference between the relay delay and actual primary rocket burn time. The nominal value of the relay time delay is the sum of  $t_d$  and  $t_p$ , 0.41 s. Assuming a normally distributed relay error of  $\pm 5\%$ , the relay standard deviation is 0.006 s. The primary rocket burn time has mean value 0.26 s with standard deviation of 0.005 s. The difference between these two is the delay time with mean value 0.15 s. The delay time standard deviation is found by taking the square root of the sum of the squares of the two variables, and is 0.008 s.

### STATISTICAL ANALYSIS

Equations (1) through (15) describe the relations between the 14 independent variables ( $L$ ,  $t_p$ ,  $R_p/M$ ,  $t_d$ ,  $\theta$ ,  $\alpha$ ,  $P_0$ ,  $NFCDS$ ,  $A_f$ ,  $t_r$ ,  $V_h$ ,  $R_s/M$ ,  $M$ , and  $t_s$ ) and the 9 dependent variables ( $H_0$ ,  $H_1$ ,  $H_2$ ,  $H_3$ ,  $V_0$ ,  $V_2$ ,  $V_3$ ,  $t_i$  and  $V_i$ ). Each independent variable has been described with a mean value and two extrema; a statistical distribution has been assumed for each. A statistical analysis is necessary to find the mean value and statistical variation of the 9 dependent variables.

A similar statistical analysis in reference 7 was performed in which the variances for the dependent variables were calculated according to special rules for combining errors found in Beers' Introduction to the Theory of Error.<sup>20</sup> These rules covered the calculation of the standard deviation of the sum or difference of variables, the product or quotient, and the product of variables raised to various powers. This approach was initially used in this study but had to be abandoned for two reasons. First, due to the complex nature of the functions for  $V_2$  and  $H_2$ , the type of distribution of  $H_2$  and  $V_2$  was unknown. Secondly, once a mean and standard deviation of  $H_2$  and  $V_2$  were calculated, the extreme variations (we assumed a normal distribution for  $H_2$  and  $V_2$  for this approach) could not be related to each other. In other words, for the extreme case where  $H_2$  is by chance  $2\sigma$  above its mean value, is  $V_2$  also  $2\sigma$  above its mean value? Since  $H_2$  and  $V_2$  both depend on the same variables due to one being the time derivative of the other, this seems like a plausible assumption. It is important to know this to describe the worst cases which will determine the feasibility of retrorocket soft landing. The answer is "not necessarily." Twenty-seven example cases were

<sup>20</sup>Y. A. Beers. Introduction to the Theory of Error, Addison Wesley, 1953

examined where independent variables directly affecting  $H_2$  and  $V_2$  were systematically varied. Variables  $V_0$ ,  $R_p/M$  and  $t_p$  were each given 3 values: Mean  $-2.58\sigma$ , mean, and mean  $+2.58\sigma$ . Values of load height and velocity after burnout,  $H_2$  and  $V_2$  were found by evaluating equations (5) and (6) for all combinations of the 3 values of the 3 variables, twenty-seven cases in all. There was a basic trend toward the  $H_2$ ,  $V_2$  pair deviating identically from the respective means, but several cases showed extremes such as  $H_2$  above its mean by  $1.25\sigma$  when  $V_2$  was  $0.7\sigma$  below its mean. As a result of these problems, a different approach was devised. On a large UNIVAC computer a random number generating program was used to generate 500 random values for each of the 14 independent variables according to their distribution. For each of these 500 sets, all 9 dependent variables were computed, resulting in 500 different soft landing cases. A flowchart of the computer program is shown in Figure 5. The dependent variables were then analyzed in a statistical computer program, BMDP2D,<sup>21</sup> which plotted a histogram, calculated mean values and standard deviations, and generated a frequency table showing the cumulative dependent variable value in 0.2% divisions from 0 to 100.

Many of the variables, both independent and dependent, are a function of temperature. To keep the independent variables independent, the temperature variation was factored out, and the statistical analysis was performed for a specific temperature. Extreme values of  $T$  are 233 K ( $-40^\circ\text{F}$ ) to 311 K ( $100^\circ\text{F}$ ), with a standard value of 288 K ( $59^\circ\text{F}$ ). There are three variables which need to be adjusted so that certain criteria are satisfied.

First,  $L$  must be chosen so that  $H_2$  at the 2.5 percentile at  $T = 311$  K is approximately zero. This is necessary so that in design condition 1, the worst case of fast descent with minimal thrust, burnout occurs at or just prior to impact.

Second,  $t_p$  is chosen so impact velocity at the temperature extremes of 233 K and 311 K is minimized and is approximately the same. This is done by trial and error.

Third,  $t_d$  is chosen to be somewhat less than the time to reduce  $V_2$  at the 2.5 percentile at  $T = 233$  K to zero. This is the worst case of velocity reversal where load velocity at burnout,  $V_2$ , is a maximum value upward. A value of  $t_d$  which would allow  $V_2$  to decrease to zero would minimize  $V_i$  at the 2.5 percentile, but would cause an unacceptable increase in  $V_i$  at the 97.5 percentile. A value of  $t_d$  which is about 70% of this value appears to be a good trade-off.

In the computer program there are cases where impact occurs during the delay period. When this occurs,  $H_3$ , the load height after the end of the delay period, will have a negative value. In the program there is a test of the value of  $H_3$ ; if it is negative the value of  $V_i$  is calculated according to the time the load free falls after primary rocket burnout. Thus the variable  $t_j$  has a dual definition as shown in Figure 5.

<sup>21</sup> BMDP2D, Frequency Count Routine; Biomedical Computer Programs, University of California Press, Berkeley, CA, 1975

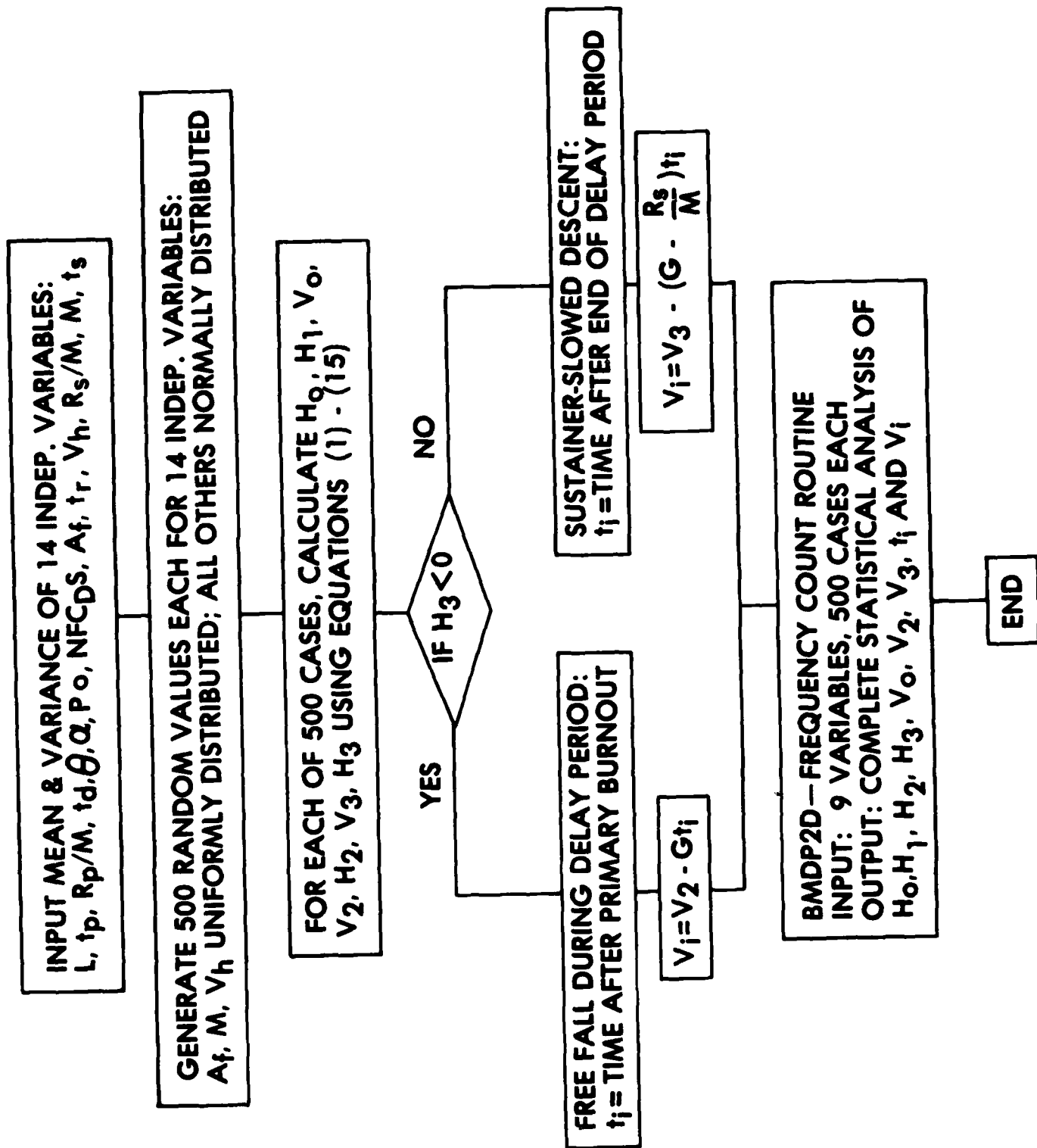


Figure 5. Computer Program Flowchart

## RESULTS AND DISCUSSION

One of the benefits inherent in a retrorocket soft landing system is the fact that the temperature effects of the two most important factors are similar. In Figure 6 the temperature variation of descent velocity  $V_0$  and retrorocket impulses  $R_{ptp}$  and  $R_{sts}$  are plotted. Impulse is thrust multiplied by burn time; although rocket thrust varies with temperature in the opposite manner to burn time, the product of these two, the total work done by the rockets, is the main consideration. At the colder ambient temperatures, the total work done by the rockets is reduced, but the lower load descent velocity requires less work to be exerted by the rockets, and vice-versa at the higher ambient temperatures. Although the percentage change of impulse and descent velocity with temperature is not identical, it is of the same sense, which helps to reduce the temperature variation of impact velocity.

### Effect of Selected Variables

The 17 variables can be divided into three groups. The first group is made up of the five basic system variables:  $M_{sm}$ ,  $R_p/M$ ,  $R_s/M$ ,  $M$ , and  $L$ . These variables have values or standard deviations set by basic system components such as the parachute system, primary and sustainer retrorocket system, system minimum mass, and type of ground sensor. The second group consists of atmospheric and terrain-related variables:  $A_f$ ,  $V_h$ ,  $T$ ,  $T_p$ ,  $\alpha$ , and  $P_0$ . The limits of these variables were chosen as reasonable extremes that an airdrop system may be expected to encounter. Reduction in the limits of these variables will reduce the operational envelope and thereby may restrict the ability to carry out the airdrop mission. The third group consists of variables that have relatively fixed standard deviations:  $NFCDS$ ,  $\theta$ ,  $t_p$ ,  $t_r$ ,  $t_s$ , and  $t_d$ . These variables have an inherent variation, estimated for each variable in a previous section of this report. Unless a reasonable change to these estimated limits of variation can be justified, this third group of variables has fixed standard deviations. In the statistical analysis, the values of the 14 independent variables used to calculate the impact velocity were generated by the computer within the distributions specified. The individual effect of each variable on impact velocity was therefore masked. In this section, each variable in the first group, i.e., the basic system variables, will be examined for the individual effect on impact velocity. It is these variables which would be modified to make any improvements in the system.

#### (a) System Minimum Mass ( $M_{sm}$ ), Primary Thrust/Mass Ratio ( $R_p/M$ ), and Sustainer Thrust/Mass Ratio ( $R_s/M$ )

The system minimum mass is the mass of the lightest item to be airdropped by means of retrorocket soft landing. In the PRAD System, the system minimum mass was 3600 kg; loads with lower mass (900 to 3600 kg) were to be airdropped with parachutes only. In a retrorocket system where a certain number of specific sizes of retrorockets and parachutes are affixed to a load, having small load masses makes it difficult to achieve the nominal descent rate and rocket thrust desired. The thrust/mass ratio experiences the greatest variation with the smallest masses due to the small denominator in comparison to the fixed-increment numerator. The effect of the system minimum mass on the primary rocket thrust/mass ratio  $R_p/M$ , and the sustainer rocket thrust/mass ratio,  $R_s/M$  is shown in Table 10.

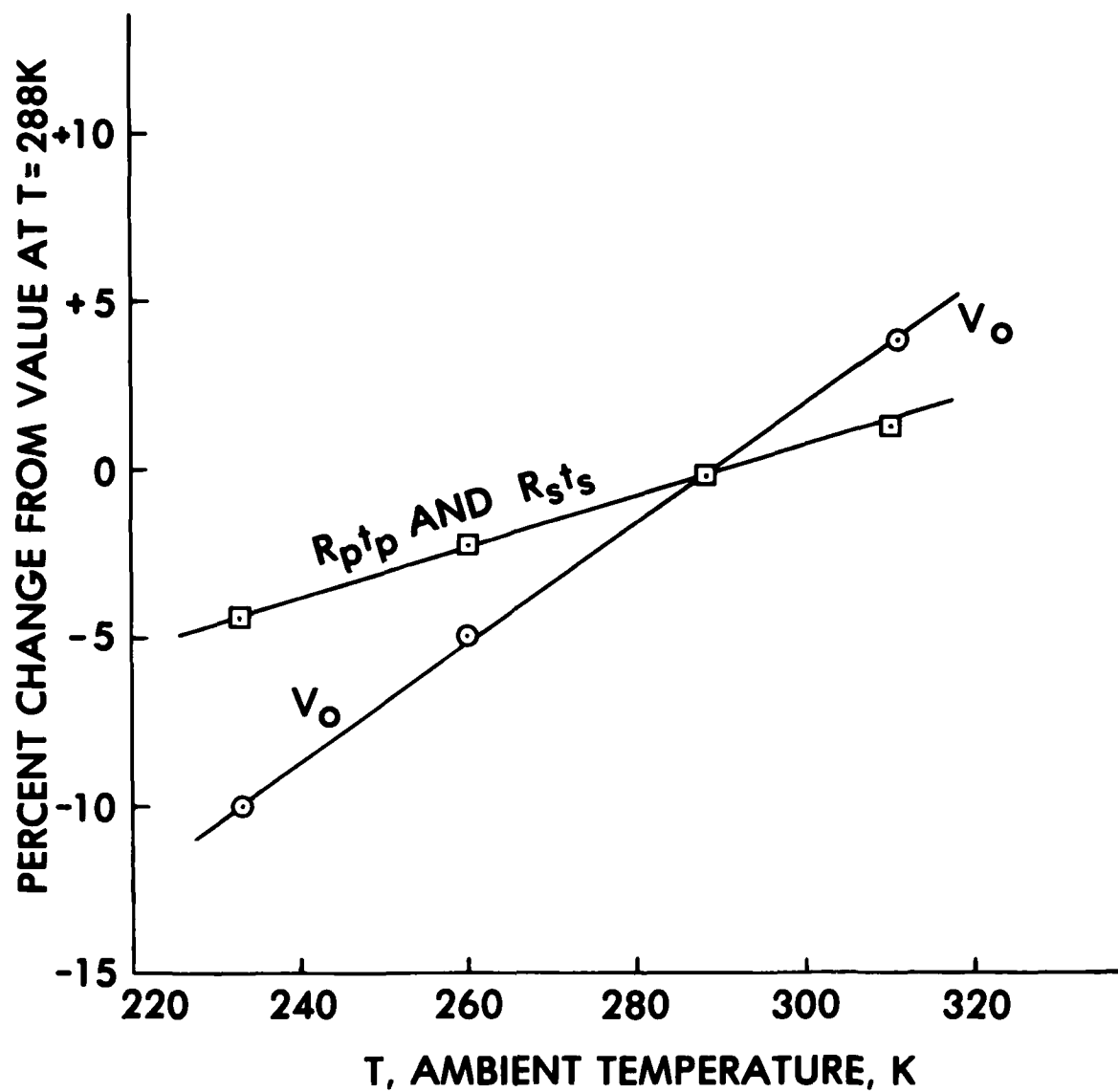


Figure 6. Percent Change of Descent Velocity,  $V_o$  and Rocket Impulses  $R_{ptp}$  and  $R_{sts}$ , with Temperature



Table 10

## System Minimum Mass

System Designation	System Minimum Mass, $M_{sm}$		R <sub>p</sub> /M Range		R <sub>s</sub> /M Range		Standard Deviations	
	(kg)	(lb)	From (G)	To (G)	From (G)	To (G)	R <sub>p</sub> /M (G)	R <sub>s</sub> /M (G)
I	900	1980	7.99	6.00	0.84	0.56	0.29	0.040
II	1364	3000	7.64	6.37	0.81	0.60	0.18	0.032
III	1900	4180	7.52	6.53	0.78	0.62	0.15	0.022
IV	2272	5000	7.41	6.59	0.78	0.64	0.12	0.022
V	2770	6100	7.36	6.67	0.76	0.64	0.10	0.017
VI	3180	7000	7.30	6.70	0.75	0.64	0.09	0.014

For system I, the variation of  $R_p/M$  is 6.00 to 7.99 G, a variation of approximately  $\pm 1$  G about the chosen value of 7.0 G. By raising the system minimum mass to that of system VI, the variation of  $R_p/M$  is reduced to  $\pm 0.3$  G, which is better than a 3-to-1 reduction. A similar reduction in variation is realized in the variable  $R_s/M$ . The effect of these various minimum masses on the impact velocity is shown in Figure 7. In this figure the statistical distribution of impact velocity, i.e., the maximum, minimum, mean, and several percentiles are given as a function of minimum load mass. The standard deviation data from Table 10 was the only parameter changed in the 500-case computer statistical analysis, run for systems I, II, IV, and VI. The 0 and 100 percentile curves represent the minimum and maximum cases of the 500 cases run, and are the extremes of impact velocity expected in 500 soft landings. A different sample size (i.e., number of cases) would give slightly a different impact velocity for all percentiles, but the 0 and 100 percentiles would be most affected. From Figure 7 it is seen that the mean value of impact velocity decreases slightly from system I to system VI, approximately 7 percent. The impact velocity range, defined arbitrarily to be the range bracketed by the 2.5 and 97.5 percentiles, decreases by 24% from system I to VI.

The retrorocket system, of course, is the main factor in determining  $\sigma_{R_p/M}$ , the standard deviation of  $R_p/M$ . The retrorocket system chosen for this study (see Table 3), requires only three sizes of primary rockets up to a mass of 16,700 kg (36,740 lb). If two sizes or four sizes were chosen, a different value for  $\sigma_{R_p/M}$  would result. It was found that the changes in impact velocity shown in Figure 7 are almost completely due to the variation in  $\sigma_{R_p/M}$ ; variation of  $\sigma_{R_s/M}$  has a very minor effect on impact velocity.

#### (b) Load Mass, M

The choice of a parachute system determines the mass ranges and sets the value for the standard deviation of mass,  $\sigma_M$ . As seen in Table 4, a load having a mass in the exact center of a mass range will result in descent velocity,  $V_0$ , of 16 m/s in a standard atmosphere. A load with mass other than the range median will have a descent velocity which deviates from the chosen value. The value of  $\sigma_M$  is dependent on only the size of the mass range. For this study the example case of  $M = 2975$  kg and  $\sigma_M = 187.6$  kg was used. If a parachute system with fewer parachute sizes was used (3 instead of 4, for example) the load mass ranges would increase and so would  $\sigma_M$ . The effect of a 50% increase in  $\sigma_M$  is to increase the range of descent velocity by 26% and to increase the mean impact velocity by 6%.

#### (c) Probe Length, L

The accuracy of the means of sensing the distance L above the ground depends on the method used. The rigid probe used in reference 7 was about twice as accurate as the crossed-beam laser device used in PRADS. In this study the value of  $\sigma_L$ , the standard deviation of L, was chosen to be approximately the average of the two above methods. A doubling of  $\sigma_L$  from 29 mm to 58 mm did not change the mean value of impact velocity and increased the range of impact velocity by only 2%, a change having surprisingly minor consequences. This doubling of  $\sigma_L$  in effect increased the variation of L from  $3.42 \pm 0.1$  m to  $3.42 \pm 0.2$  m. The system is not sensitive to changes of this magnitude.

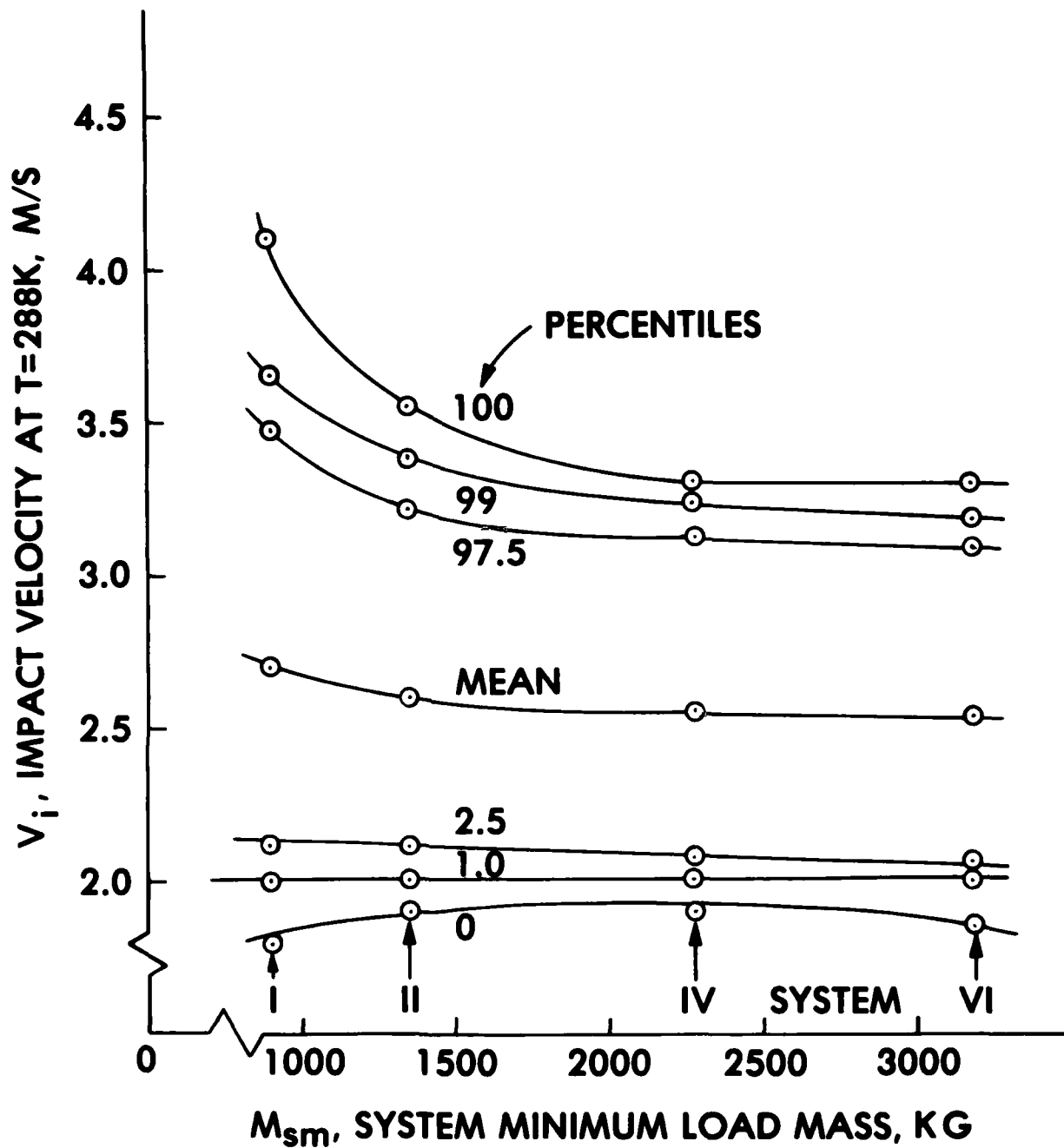


Figure 7. Effect of System Minimum Load Mass on Impact Velocity for  $T = 288\text{ K}$

## Sustainer Rocket Burn Time

The burn time of the sustainer rocket needs to be as long as necessary to soft land the worst case of velocity reversal. The variable  $t_i$  is the time from sustainer rocket ignition to impact, or if impact occurs during the delay period, it is the time from primary rocket burnout to impact. Values of  $t_i$  are shown for four systems at the two temperature extremes, in Table 11.

Table 11

### Impact Time $t_i$

System Designation	Time to Impact from Sustainer Rocket Ignition or Primary Rocket Burnout, (s)					
	Mean	T = 233 K		Mean	T = 311 K	
		99 Percentile	Max		99 Percentile	Max
I	0.35	1.09	1.63	0.16	0.78	1.44
II	0.34	0.92	1.34	0.15	0.65	1.10
IV	0.34	0.93	1.19	0.15	0.69	0.93
VI	0.35	0.96	1.13	0.15	0.71	0.86

For a given system, there is a considerable difference in  $t_i$  between the 99th percentile and the maximum values. For example, in system II a value of sustainer rocket burn time of 1.34 s will be long enough to soft land all 500 of the soft landing cases run on the computer for the extreme temperature of 233 K. However, only 1% of the cases require more than 0.92 s burn time. It is felt that the 31% reduction in burn time, and therefore in propellant and the weight of the propellant, is a good trade-off for slightly increased impact velocity in the statistically extreme cases. From Table 11 it is seen that approximately a 1.1 s sustainer rocket burn time will cover 99% of all soft landings at  $T = 233$  K, and greater than 99% at all other temperatures.

### Histograms of Variables

In the statistical analysis, the independent variables were assumed to have either a normal or uniform distribution. The computer used internal random number generating programs to create 500 random values for each variable in accordance with the distribution, mean and standard deviation specified. For two of these independent variables,  $M$  and  $R_p/M$ , the 500 computer-generated values were then statistically analyzed to see if the specified and actual mean and standard deviations agreed. Table 12 shows the results:

TABLE 12

Comparison of Statistical Parameters for Load Mass (M) and  
Primary Rocket Thrust/Mass Ratio, ( $R_p/M$ )

	M (kg)	$\sigma_M$ (kg)	$R_p/M$ (m/s <sup>2</sup> )	$\sigma_{R_p/M}$ (m/s <sup>2</sup> )
Specified Value	2975.0	187.6	68.6	2.8
Statistical Analysis of 500 Random Values	2981.1	188.4	68.58	2.72

From Table 12 it is seen that the statistical mean and standard deviation of the 500 random values are in very close agreement with the specified values.

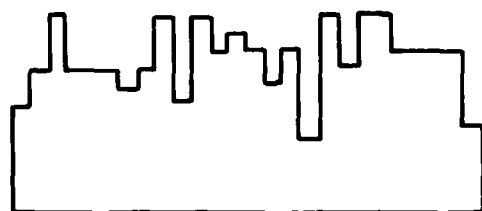
The histograms of M and  $R_p/M$  are shown in Figure 8, along with histograms of four example dependent parameters: velocity and height after primary rocket burnout  $V_2$  and  $H_2$ , impact velocity  $V_i$  and time from either primary rocket burnout (or sustainer rocket fire) to impact,  $t_i$ . These four parameters are computed from a mixture of normally and uniformly distributed independent variables using equations (1) through (15). Included in the figure are values of skewness and kurtosis for each distribution, measures of departure of the distributions from normality. Skewness is a measure of asymmetry about the mean. A value of zero indicates perfect symmetry about the mean, while a plus value indicates skewness to the right. Kurtosis is a measure of long-tailedness of the distribution curve. A value of zero indicates a normal curve, a positive value usually indicates an excess of values near the mean giving the distribution a sharper peak, and a negative value indicates a long-tailed or flat-topped distribution curve. The distribution curve for M was specified to be uniform, not normal, so the large, negative value for kurtosis is fully expected. The distributions for  $V_2$ ,  $H_2$  and  $V_i$  are very nearly normal, but that for  $t_i$  is nearly exponential. The exponential shape of the  $t_i$  distribution is due in part to its dual definition.

The distributions in Figure 8 are typical for an ambient temperature of 288 K (59°F). For lower temperatures the skewness and kurtosis of  $V_i$  become more negative and more positive, respectively. For higher temperatures, just the opposite takes place.

#### Impact Velocity

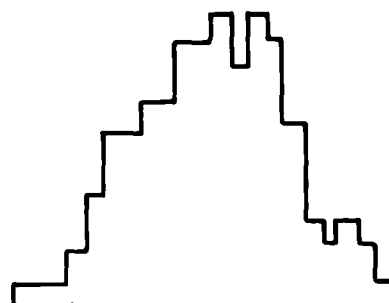
To achieve perfect soft landing two criteria must be met. First the retrorocket impulse must be exactly right to reduce load descent velocity to zero. Secondly, the ignition altitude must be proper so the height at rocket burnout is zero. If only one of these criteria is satisfied, a nonzero impact velocity will result.

Design condition 1 represents the case where descent velocity is high and thrust is low. The ignition height,  $H_0$ , for this extreme case must be relatively high to assure rocket burnout



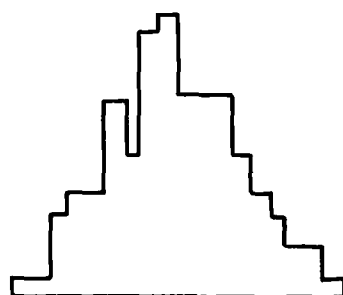
$M$

$S = -.06$     $K = -1.21$



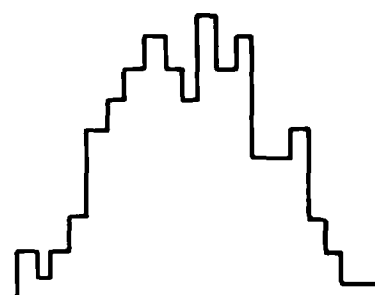
$R_p/M$

$S = .003$     $K = -.24$



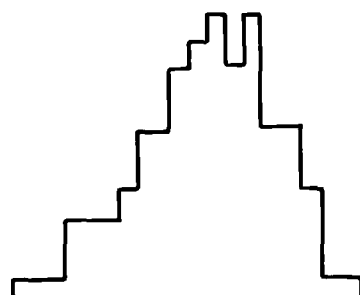
$V_2$

$S = .07$     $K = .05$



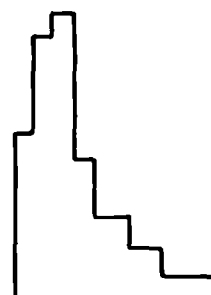
$H_2$

$S = -.05$     $K = -.29$



$V_i$

$S = -.54$     $K = .16$



$t_i$

$S = 2.0$     $K = 5.7$

Figure 8. Frequency Histogram of Variables for System I with  $T = 288$  K, Including Skewness (S) and Kurtosis (K) Values

at or before impact. Since the system employs a fixed-height ground sensor, the system value of  $H_0$  is set by this condition. The procedure used is to assume a value for  $H_0$ , run a 500-case statistical analysis for an ambient temperature of 311 K (descent velocity is highest for this upper temperature limit), and observe the 2.5 percentile value of the height at rocket burnout,  $H_2$ . The value of  $H_2$  at the arbitrarily chosen 2.5 percentile level should be zero, and a trial and error procedure is used to determine the value of  $H_0$  to achieve this. The value of  $H_2$  determined in this way was 3.42 m; at the extreme case when  $T = 311$  K ( $100^\circ\text{F}$ ), 97.5% of all soft landings are expected to have burnout at or before impact. At lower ambient temperatures this percentage increases to 100%.

The rockets attached to a load are based upon an average descent velocity; at the high descent velocity at design condition 1, the rocket thrust is too low to reduce descent velocity to zero. In fact, the lowest impact velocity possible at design condition 1 is approximately 2.5 m/s.

Design condition 2 represents the case where descent velocity is low and thrust is high. The value of  $H_0$  as set by the opposite extreme (design condition 1) is much too high for this case. To further complicate matters, the excessive thrust causes the load to reverse direction and climb upward. Neither perfect soft landing criterion is met here; the load cannot soft land with zero velocity.

With the ideal zero-velocity soft landing not possible at the two extremes, design condition 1 and 2, is it possible at some point in between? The answer is no, due to the value of  $H_0$  being too high. The necessity of setting  $H_0$  high enough to satisfy design condition 1 precludes the possibility of a zero velocity throughout the entire system.

Figures 9 through 12 show the impact velocity as a function of ambient temperature for soft landing systems I, II, IV and VI. The 0 and 100 percentile values are the two extremes of the 500 cases run; due to the finite, moderate sample size (500) these percentiles should not be interpreted as absolute extremes. Comparison of systems I and VI (Figures 9 and 12) reveals the decrease in range of impact velocity due to increasing the system minimum mass from 900 kg to 3180 kg. This is due to a decrease in the high percentile values while the low percentile values remain virtually unchanged, as previously seen in Figure 7. The effect of temperature is interesting; at temperatures near that of the standard atmosphere, 288 K ( $59^\circ\text{F}$ ), the range of impact velocities is minimized. At temperatures higher or lower, the range of impact velocities increases. Temperature affects five variables:  $V_0$ ,  $R_p$ ,  $t_p$ ,  $R_s$ , and  $t_s$ . The difference in temperature variation of  $V_0$ ,  $R_p t_p$  and  $R_s t_s$ , as previously shown in Figure 6, accounts for the variation of impact velocity with temperature.

In all the soft landing systems some skewness in the impact velocity distribution is apparent, but it is most pronounced at lower temperatures and in system I. In this system at  $T = 233$  K the impact velocity range is approximately 2 to 5 m/s, but only 1% of impact velocities occur in the upper third of the range, between 4 and 5 m/s.

For all four systems shown in Figures 9–12, the mean impact velocity is below 3 m/s. In a preceding section of this report, a practical estimate of maximum allowable impact velocity was given in terms of a range, 3.0 to 3.5 m/s. In Figures 9–12 it is not clear quantitatively

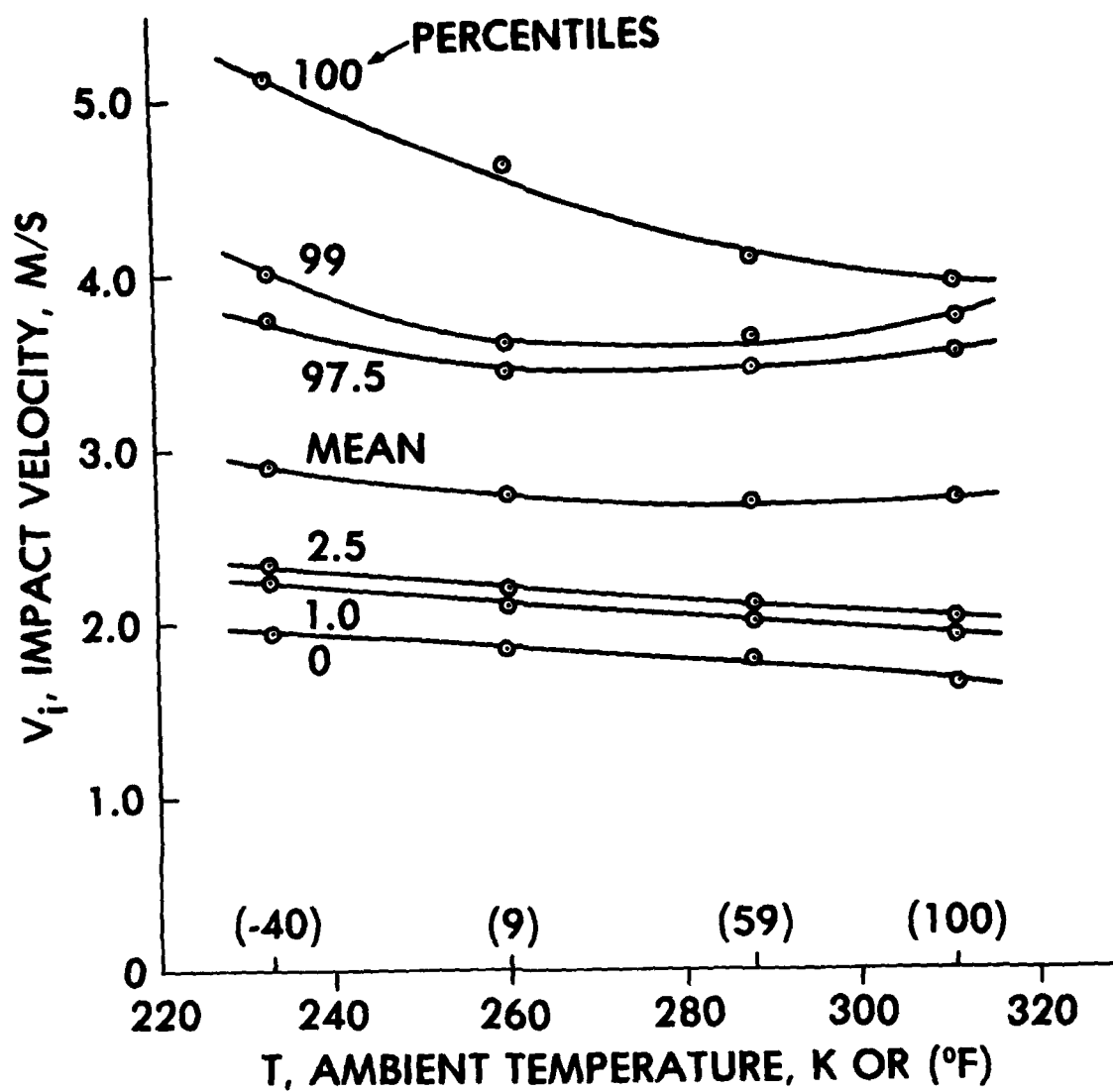


Figure 9. Soft Landing System I, 900–25,000 kg



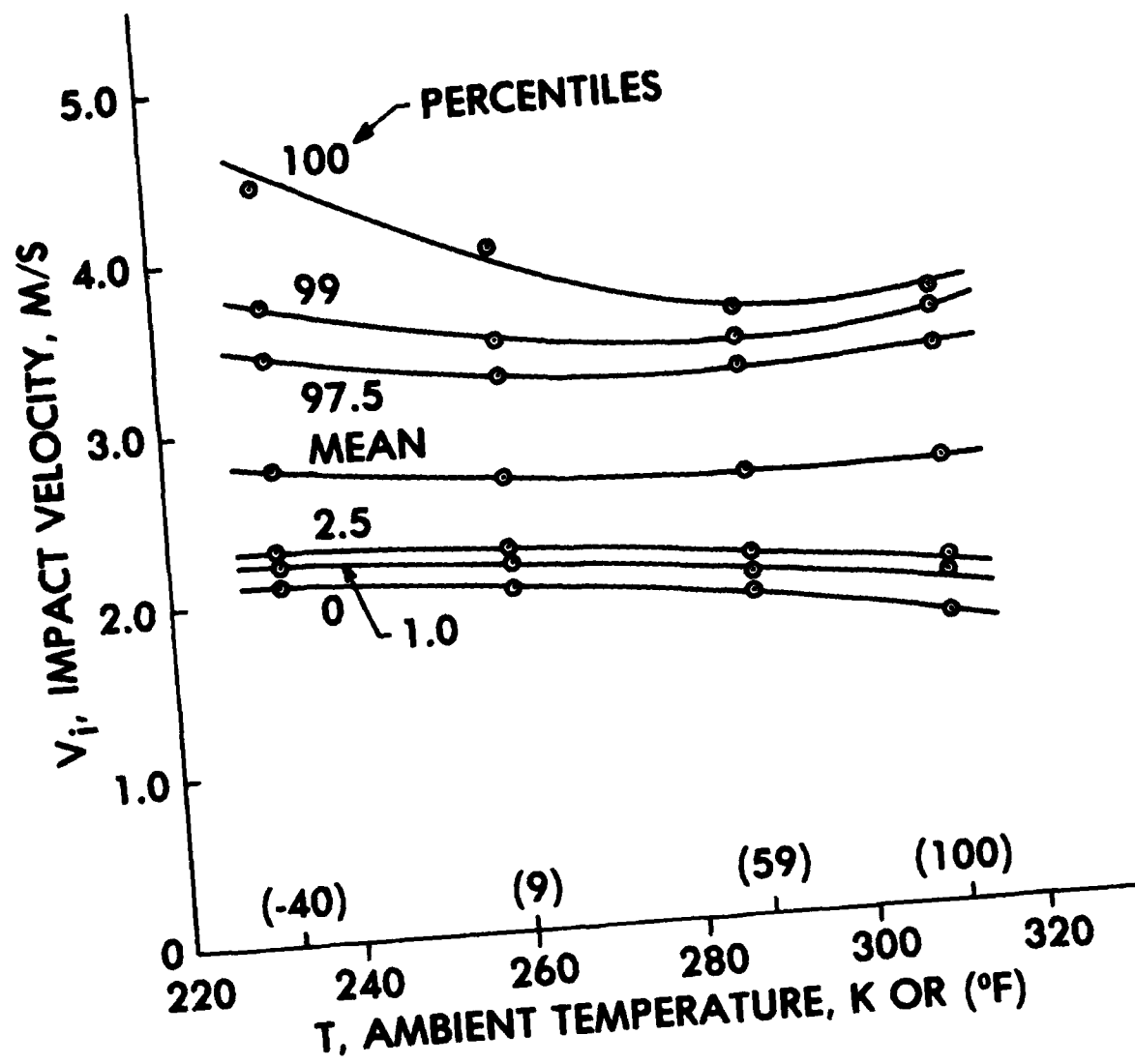


Figure 10. Soft Landing System II, 1364–25,000 kg

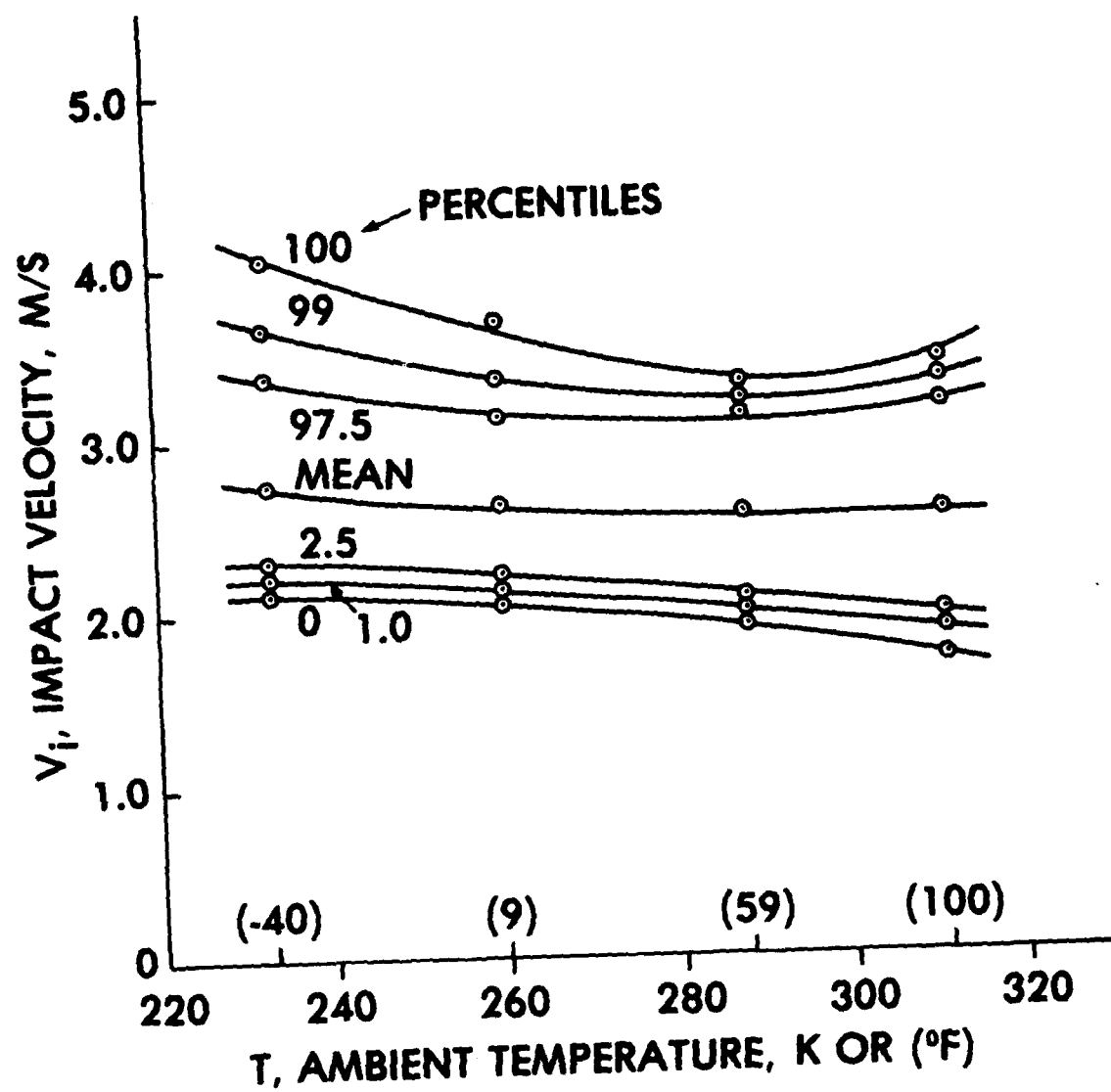


Figure 11. Soft Landing System IV, 2272–25,000 kg

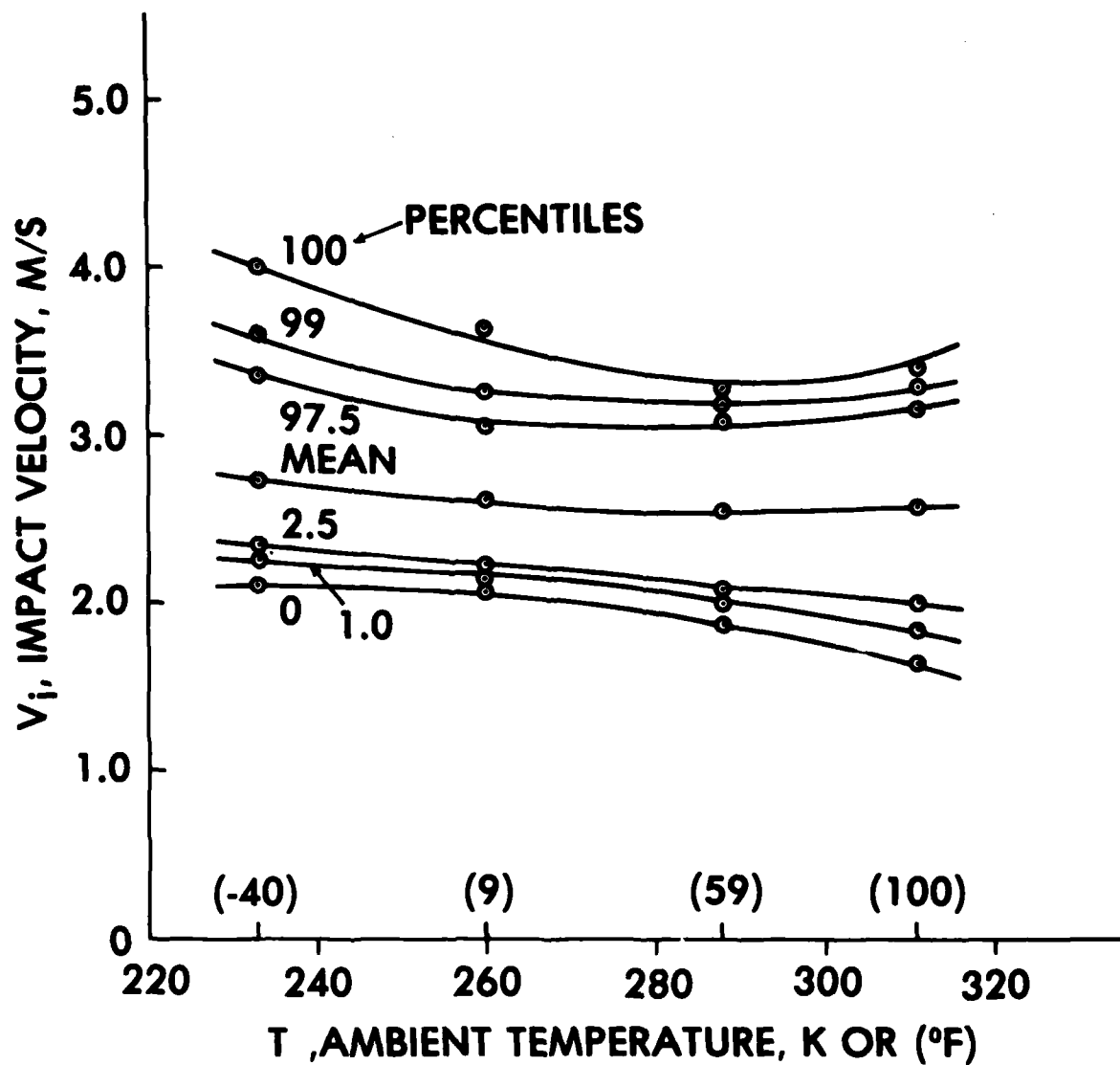


Figure 12. Soft Landing System VI, 3180–25,000 kg

how the various systems compare to this estimate. For the four systems, the percentage of impacts greater than 3.0 and 3.5 m/s is listed in Table 13. Percentages in this table are based upon 500 sample cases run through the statistical analysis.

If the maximum no-damage impact velocity of 3.5 m/s is assumed, and system I is chosen:

(a) Mean impact velocity would be 2.9 m/s maximum, equivalent to a free fall of 0.43 m (16.9 in).

(b) Above 250 K ( $-9^{\circ}\text{F}$ ), 97.5% of all impacts would be expected to have velocities below 3.5 m/s.

(c) System minimum load mass would be 900 kg (2000 lb), the same as in the present system.

Table 13

Percentage of Impacts Greater Than 3.0 and 3.5 m/s

System	Percent Impacts > 3.0 m/s at Temperature (K) of				Percent Impacts > 3.5 m/s at Temperature (K) of			
	233	260	288	311	233	260	288	311
I	32.6	21.6	19.8	22.0	5.0	2.2	1.8	2.8
II	20.0	11.4	11.8	15.2	2.2	0.8	0.2	0.8
IV	15.4	6.0	6.2	9.0	1.4	0.6	0.0	0.0
VI	12.8	4.4	4.8	6.4	1.2	0.4	0.0	0.0

If system II is chosen:

(a) Mean impact velocity would be 2.8 m/s maximum, equivalent to a free fall of 0.40 m (15.7 in).

(b) Above 250 K, 99% of all impacts would be expected to have velocities below 3.5 m/s.

(c) System minimum load mass would be 1364 kg (3000 lb).

There are many ways one can tailor the system to achieve desired results once an upper limit to impact velocity is established. The differences between systems I and II as listed above are solely the result of increasing  $M_{sm}$  from 900 kg to 1364 kg. Varying the retrorocket systems or the parachute systems so as to reduce the standard deviation of  $M$ ,  $R_p/M$ , or  $R_s/M$ , would also reduce the magnitude of impact velocity.

### CONCLUSIONS

1. A soft landing system (system II) comprised of
  - (a) Load mass range 1364–25,000 kg (3000–55,000 lb)
  - (b) Nominal descent rate of 16 m/s achieved by clustering from 3 to 6 of four sizes of parachutes
  - (c) Ground height sensor length 3.4 m with  $\pm 0.1$  m accuracy
  - (d) Primary rocket nominal thrust/mass ratio of 7 G achieved by up to 12 rockets of 4 sizes, burn time 0.26 seconds
  - (e) Delay after primary burnout 0.15 seconds
  - (f) Sustainer rocket nominal thrust/mass ratio of 0.7 G achieved by up to 12 rockets of 2 sizes, burn time 1.1 seconds,descending to a drop zone which is between 0 and 1524 m above sea level, in winds between 0 and 10 m/s, experiencing up to  $\pm 10^\circ$  system oscillations, and landing on terrain with slopes  $\pm 5^\circ$  from the horizontal, statistically will achieve a mean impact velocity at 288 K (59°F) of 2.6 m/s, with 95% of soft landings over the temperature range 233 to 311 K expected to have impact velocities between 2.0 and 3.4 m/s. Systems with greater minimum masses will have lower impact velocities and vice-versa.
2. A zero-velocity soft landing is not possible due to the constraint of fixed-height ground sensing and no primary rocket burn after impact under all conditions.
3. The judgment of the successfulness of this soft landing system has to be primarily based on a quantity that is presently unknown — the fragility of uncushioned airdropped items. If it is determined that all airdropped items can withstand repeated impacts of 3.5 m/s without damage, the soft landing system outlined in this study is successful in theory; for system II at temperatures above 250 K ( $-9^\circ\text{F}$ ), less than 1% of impacts are expected to have velocity greater than 3.5 m/s. The reduction of this soft landing system to practice, based upon work done in PRADS and the B-1 Emergency Escape Module, appears to be within the state of the art.

## REFERENCES

1. Litz, C. J., Jr.; Propellant Actuated Device (PAD) Assisted Parachute System for Aerial Delivery of Cargo. Frankford Arsenal, Philadelphia, PA, NARADCOM Project Order QMREC-62-53, March 1963 (AD 415 227).
2. Neuwien, R. A., Jr.; An Engineering Evaluation Test of the Rocket Assist Parachute System for Airdrop of Cargo (Phase II - Live Rockets), USATECOM Project 4-3-7270-01, YTS Report 3054, Yuma Test Station, Yuma, AZ, August 1963
3. Michal, J. L.; Final Engineering Report - Ground Proximity Airdrop System. Stencel Aero Engineering Corp., US Army Natick Research & Development Command, Technical Report 68-71, September 1966 (AD 837 338)
4. White, E., C. Bronn, and R. Sturgeon; Study of Heavy Equipment Aerial Delivery and Retrieval Techniques. Lockheed-Georgia Co., Contract No. AF33(615)-2989, Air Force Flight Dynamics Laboratory, Wright Patterson AFB, Ohio, AFFDL-TR-66-97, 1967 (AD 810 301)
5. Michal, J. L., J. L. Oates, and A. L. Martinez; Final Engineering Report - Parachute Retrorocket Airdrop System. Stencel Aero Engineering Corp., US Army Natick Research & Development Command, Technical Report 72-16, December 1970 (AD 736 361)
6. Chakoian, G.; A Parachute Retrorocket Recovery System for Airdrop of Heavy Loads, US Army Natick Research & Development Command, Technical Report 70-34-AD, November 1969 (AD 699 342)
7. Babish, C. A., et al; A Parachute/Retrorocket Landing System for Aeronautical Vehicles - Study of System Applicability to the B-1 Aircraft Emergency Crew Escape Module. AFFDL-TR-77-140, Air Force Flight Dynamics Laboratory Wright Patterson AFB, Ohio, February 1978
8. Army Technical Bulletin TB-381-5-11, Foreign Materiel Catalog, Volume 11, Aerial Delivery Equipment, Class 1670, Headquarters, Department of the Army, September 1977
9. Chakoian, G.; Plan for Advanced Development of a Parachute Retrorocket Airdrop System. NARADCOM TR-73-59-AD, US Army Natick Research & Development Command, Natick, MA, May 1973 (AD 765 422)
10. Automotive Bodies and Hulls, AMC Pamphlet 706-357, April 1970
11. Covington, C. and R. Shield; Fragility Studies, Part II, Truck, Cargo, M-37, 3/4-Ton. University of Texas Structural Mechanics Research Laboratory, Austin, TX, April 1960
12. Ripperger, E. A.; Impact Determinations, Final Report. University of Texas Structural Mechanics Research Laboratory, Austin, TX, 1962 (AD 400 638)

13. Ripperger, E. A.; Ground Impact Shock Mitigation. Engineering Mechanics Research Laboratory, University of Texas, Austin, TX, 1967 (AD 830 179)
14. Military Specification MIL-C-25969 (USAF), Capsule Emergency Escape Systems, General Requirements For, 4 March 1970
15. Wine, R. L.; Statistics for Scientists and Engineers. Prentice Hall, Englewood Cliffs, NJ, 1964
16. Handbook of Geophysical & Space Environments. Air Force Cambridge Research Laboratory, USAF, 1965
17. Engineering Design Handbook, Design for Air Transport and Airdrop of Materiel. AMC Pamphlet 706-130, HQ, US Army Materiel Command, Washington, DC, December 1967
18. Warren, F. A.; Rocket Propellants. Reinhold Publishing Corp., New York, NY, 1958
19. Clark, J. F., Jr.; Development of Rocket Motor for Parachute Retrorocket Airdrop System. Frankford Arsenal, Philadelphia, PA, June 1973
20. Beers, Y. A.; Introduction to the Theory of Error. Addison-Wesley, 1953
21. BMDP2D, Frequency Count Routine; Biomedical Computer Programs, University of California Press, Berkeley, CA, 1975
22. Dommasch, D., S. Sherby and T. Connolly; Airplane Aerodynamics, 3rd Edition. Pitman Publishing Co., New York, NY, 1951
23. Performance of and Design Criteria for Deployable Aerodynamic Decelerators. Air Force Flight Dynamics Laboratory, Wright Patterson AFB, Ohio, December 1963 (AD 429 971)
24. Army FM 10-516, Airdrop of Supplies and Equipment; Reference Data for Airdrop Platform Loads, 1975

## APPENDIX A

### Derivation of Descent Velocity Equation

From Reference 17, descent velocity is defined as:

$$V_o = \left[ \frac{2MG}{\rho(NFC_D S)} \right]^{1/2} \quad (A1)$$

From Airplane Aerodynamics<sup>22</sup> air density, temperature and altitude relations in the troposphere (0 to 11,000 m) are:

$$\frac{\rho}{\rho_o} = \left[ \frac{T}{T_o} \right]^{4.2561} \quad \frac{T}{T_o} = 1 - 2.096 \times 10^{-6} h \quad (A2)$$

where  $\rho$  = air density at temperature  $T$ , kg/m<sup>3</sup>

$\rho_o$  = standard sea level air density = 1.225 kg/m<sup>3</sup>

$T$  = air temperature at altitude  $h$ , K

$T_o$  = standard sea level temperature = 288 K

$h$  = altitude above sea level, m

Note that  $\frac{\rho}{\rho_o} = \frac{T_o}{T} \left[ \frac{T}{T_o} \right]^{5.2561} = \frac{T_o}{T} (1 - 2.256 \times 10^{-5} h)^{5.2561}$  (A3)

and  $\frac{\rho}{\rho_o T_o} = \frac{\left[ 1 - \frac{h}{44334} \right]^{5.2561}}{T}$  (A4)

The geopotential equation of state is:  $\rho_o T_o = \frac{p_o}{G_o R}$  (A5)

<sup>22</sup> D. Dommasch, S. Sherby and T. Connolly; Airplane Aerodynamics, 3rd Ed., Pitman Publishing Co., New York, NY, 1951



Combine (A4) and (A5), solve for  $\rho$ : 
$$\rho = \frac{P_o}{G_o RT} \left[ 1 - \frac{h}{44334} \right]^{5.2561} \quad (A6)$$

Note  $P_o = 101.325 \text{ kPa}$

$G_o = 9.8 \text{ m/s}^2$

$R = 29.29 \frac{\text{m}}{\text{K}}$

Then 
$$\rho = \frac{P_o}{0.287T} \left[ 1 - \frac{h}{44334} \right]^{5.2561} \quad (A7)$$

and

$$V_o = \left[ \frac{2MG}{\frac{P_o}{0.287T} \left[ 1 - \frac{h}{44334} \right]^{5.2561} (NFC_{DS})} \right]^{1/2} \quad (A8)$$

simplifying:

$$V_o = \left[ \frac{0.574 \text{ MGT}}{P_o (NFC_{DS}) A_f} \right]^{1/2} \quad (A9)$$

## APPENDIX B

### Solution of Equations of Motion for Primary Rocket Deceleration — One-Body Analysis

A one-body solution to the equations of motion during primary retrorocket deceleration implies that the entire parachute/load/rocket pack system is one rigid body. This assumption permits an exact solution to the differential equation of motion.

The forces acting on the single body are the thrust and drag upward and MG downward. For a sign convention of plus downward the equation of motion is:

$$M \frac{d^2x}{dt^2} = - R_p - D + MG \quad (B1)$$

boundary conditions:

$$(a) \quad x = H_1 \text{ at } t = 0 \quad (B2)$$

$$(b) \quad \frac{dx}{dt} = V_0 \text{ at } t = 0 \quad (B3)$$

where  $M$  = mass of system, kg

$x$  = distance above ground, m

$t$  = time, s

$R_p$  = primary retrorocket thrust, N

$D$  = parachute drag force, N

$H_1$  = height above ground at start of rocket fire

$V_0$  = system vertical descent velocity, m/s

As the parachute decelerates, drag varies as:

$$D = \left[ \frac{\frac{dx}{dt}}{V_0} \right]^2 MG \quad (B4)$$

Combining (B1) and (B4):

$$\frac{d^2 x}{dt^2} = - \frac{G}{V_o^2} \left[ \frac{dx}{dt} \right]^2 - \frac{R_p}{M} + G \quad (B5)$$

Substitute  $z = \frac{dx}{dt}$ , rewrite:

$$\frac{dz}{dt} = - \left[ \frac{G}{V_o^2} \right] z^2 - \left[ \frac{R_p}{M} - G \right] \quad (B6)$$

Separate variables:

$$\frac{dz}{- \left[ \frac{G}{V_o^2} \right] z^2 + \left[ G - \frac{R_p}{M} \right]} = dt \quad (B7)$$

From integral tables:

$$\frac{dz}{bz^2 + a} = \frac{1}{\sqrt{ab}} \tan^{-1} \left[ \frac{z \sqrt{ab}}{a} \right] \quad (B8)$$

For our case, let

$$a = G - \frac{R_p}{M}$$

$$b = -G/V_o^2$$

Integrating (B7) we obtain:

$$\frac{1}{\sqrt{ab}} \tan^{-1} \left[ \frac{z \sqrt{ab}}{a} \right] + c_1 = t + c_2 \quad (B9)$$

Combine  $c_1$  and  $c_2$  into one constant,  $c$ , and solve for  $z$ :

$$z = \frac{a}{\sqrt{ab}} \tan \left[ \sqrt{ab} (t + c) \right] \quad (\text{B10})$$

Evaluate constant C using boundary condition (B3):

$$c = \frac{\tan^{-1} \left[ \frac{V_o \sqrt{ab}}{a} \right]}{\sqrt{ab}} \quad (\text{B11})$$

Remember  $z = \frac{dx}{dt}$ ; integrate (B10):

$$x = \int \frac{a}{\sqrt{ab}} \tan \left[ \sqrt{ab}(t + c) \right] dt + d \quad (\text{B12})$$

From integration tables:

$$\int \tan (p + qx) dx = - \frac{1}{q} \ln [\cos (p + qx)] \quad (\text{B13})$$

Let  $p = c \sqrt{ab}$

$q = \sqrt{ab}$

We want  $x$  to decrease in the downward direction so the sign must be reversed: and (B12) becomes

$$x = + \frac{1}{b} \ln [\cos(\sqrt{ab}(t + c))] + d \quad (\text{B14})$$

Evaluate integration constant  $d$  using (B2 and (B11)):

$$d = H_1 - \frac{1}{b} \ln \left[ \cos \left\{ \tan^{-1} \left[ \frac{V_o \sqrt{ab}}{a} \right] \right\} \right] \quad (\text{B15})$$

In summary,

$$a = (G - \frac{R_p}{M}) \quad (\text{B16})$$

$$b = -G/V_o^2 \quad (\text{B17})$$

$$c = \frac{\tan^{-1} \left[ \frac{V_o \sqrt{ab}}{a} \right]}{\sqrt{ab}} \quad (\text{B18})$$

$$\frac{dx(t)}{dt} = \frac{a}{\sqrt{ab}} \tan \left[ \sqrt{ab}(t + c) \right] \quad (B19)$$

$$x(t) = H_1 + \frac{1}{b} \ln \left[ \cos( \sqrt{ab}(t + c)) \right] - \frac{1}{b} \ln \left[ \cos \left\{ \tan^{-1} \left[ \frac{V_0 \sqrt{ab}}{a} \right] \right\} \right] \quad (B20)$$

## APPENDIX C

### Solution of Equations of Motion for Primary Rocket Deceleration - 2-Body Analysis, and Comparison with One-Body Analysis

In this analysis the parachute(s) are considered as one body, and the load plus rocket pack is the other body, as shown in Figure C1. With the convention of + being downward, the equations of motion for the two bodies are:

$$(M_c + M_i) \frac{d^2 x_c}{dt^2} = -D + \tau - GM_c \quad (C1)$$

$$M_L \left[ \frac{d^2 x_L}{dt^2} \right] = -R_p - \tau + GM_L \quad (C2)$$

$M_c$  = total parachute mass, kg

$M_i$  = included mass of parachutes, kg

$M_L$  = mass of load and rockets, kg

$x_c$  = distance above ground of center of mass of parachutes, m

$x_L$  = distance above ground of center of mass of load and rockets, m

$R_p$  = retrorocket thrust, N

$\tau$  = total suspension line tension, N

$D$  = parachute drag, N

Included mass is calculated from Performance of and Design Criteria for Deployable Aerodynamic Decelerators:<sup>2,3</sup>

$$M_i = \frac{2d^3 \rho}{3\pi^2} \quad (C3)$$

<sup>2,3</sup>Performance of and Design Criteria for Deployable Aerodynamic Decelerators, Air Force Flight Dynamics Laboratory, Wright Patterson AFB, Ohio, December 1963 (AD 429 971)

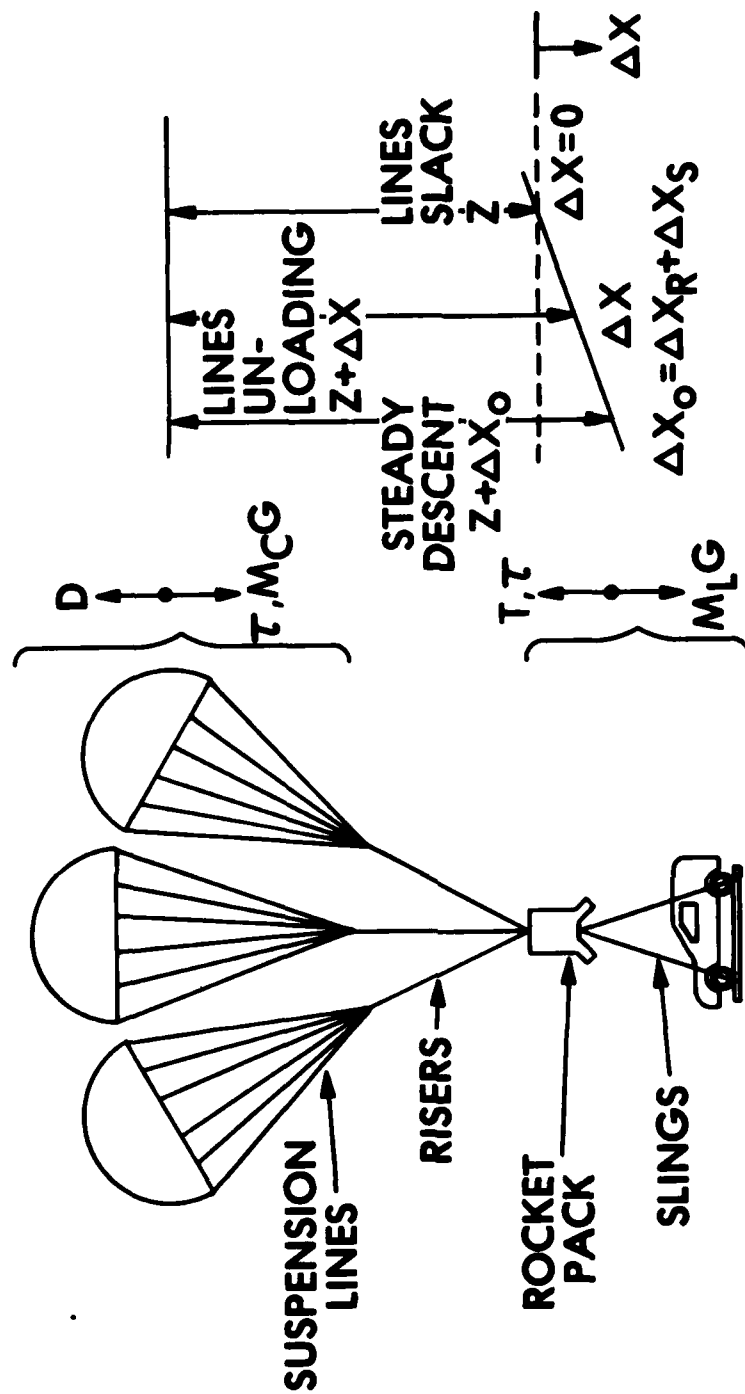


Figure C1. System Description -- Two-Body Analysis

where  $\rho$  = air density,  $\text{kg/m}^3$

$d$  = nominal parachute diameter, m

During rocket thrust, the load/rocket pack accelerates upward and moves relatively closer to the parachutes. As a result, suspension lines and risers begin to unload reducing tension  $\tau$  and the amount of line stretch. The parachutes then decelerate and drag decreases. Drag varies as:

$$D = \left[ \frac{dx_c}{dt} \right] \frac{1}{V_0} (M_c + M_i)G \quad (C4)$$

The velocity of the two bodies changes at different rates during rocket burn. The resulting difference in relative position causes the two bodies to move closer together and line tension eventually drops to zero.

The suspension lines and risers are stretched a certain amount during steady descent, and the amount of stretch depends upon the spring constant of the associated line. For a given line, a breaking strength and a percent elongation at failure can be found either in Army FM 10-516<sup>24</sup> or in the military specification for that item.

For this two-body analysis, a specific case is chosen:

Load mass	8680 kg
Parachutes	3, 19.5 m diameter (G-12)
Risers	3, 6 m long
Suspension lines	total of 192, 15.6 m long

The risers each have a steady descent tension of 28.35 kN. A typical riser for this load would be two loops of type XXVI woven nylon webbing with a breaking strength of 66.72 kN at 30% elongation. For a line length of 6 m, with four plies of woven nylon webbing, the riser spring constant,  $k$ , would be:

$$k = \frac{4(66.74)}{0.30(6)} = 148.3 \frac{\text{kN}}{\text{m}} \quad (C5)$$

<sup>24</sup>Army FM 10-516, Airdrop of Supplies and Equipment; Reference Data for Airdrop Platform Loads, 1975



This assumes linear spring behavior for the webbing, which is only an approximation of true line behavior; in actuality the time of line unloading alters  $k$  in a non-linear manner. Once  $k$  is known, the amount of line stretch for a given load can be determined by dividing the line force by  $k$ .

In our case riser line stretch during steady descent,  $\Delta x_r$ , is

$$\Delta x_r = \frac{10.48 \text{ kN}}{148.3 \frac{\text{kN}}{\text{m}}} = 0.071 \text{ m} \quad (\text{C6})$$

Suspension lines, type IV braided nylon, would typically have a breaking strength of 4448 N at 20% elongation. Line tension at steady descent would be 443 N, so the suspension spring constant  $k$  and the suspension line elongation at steady descent  $\Delta x_s$ , are

$$k = \frac{4448}{0.2(15.6)} = 1426 \frac{\text{N}}{\text{m}} \quad (\text{C7})$$

$$\Delta x_s = \frac{443}{1426} = 0.311 \text{ m}$$

During steady descent total line elongation,  $\Delta x_o$ , is

$$\Delta x_o = \Delta x_r + \Delta x_s = 0.382 \text{ m} \quad (\text{C8})$$

Referring to Figure C1,  $z$  represents the difference in position between the two bodies when  $\tau = 0$ , or the lines are slack. During steady descent the position difference is  $z + \Delta x_o$ , and during line unloading,  $0 \leq \Delta x \leq \Delta x_o$ .

Since linear spring behavior of suspension lines and risers is assumed,  $\tau$  can be calculated as

$$\tau = M_L G \left[ \frac{\Delta x}{\Delta x_o} \right] \quad (\text{C9})$$

When the two bodies move closer together a distance  $\Delta x_o$ ,  $\Delta x$  becomes 0 and so does  $\tau$ . When  $\tau = 0$ , parachute drag is ignored. In practice, parachutes can be disconnected from the load using standard ground disconnect parachute releases.

Equations (C1) and (C2) were integrated numerically using the rectangular rule with a  $\Delta t$  of 0.002 seconds. A comparison between the two-body and one-body solutions is shown in Table C1. The primary difference between the two analyses lies in the way parachute drag is accounted for. In the one-body analysis, drag is computed as in equation (C4) and does not become zero until the system velocity is zero. In the two-body analysis, the drag force is coupled to the load through line tension,  $\tau$ . As seen in equation (C9)  $\tau$  varies directly with the change in position between the two bodies. When the position change exceeds  $\Delta x_o$ ,

the line stretch at steady descent, line tension  $\tau$  becomes zero and the two bodies are decoupled. As seen in Table C1 the line unloading only takes 0.116 seconds. In our example case G-12 parachutes were chosen. If a stronger parachute is needed for this heavy loading situation, and stronger suspension lines with a higher spring constant are used, the unloading will take place in a slightly shorter time.

Referring again to Figure C1, the altitude and velocity difference between the two analyses at  $t = 0.25$  s (burnout) is insignificant. In this study, use of the one-body analysis with an exact solution of the differential equations does not introduce significant errors.

Table C1

Comparison of One-Body and Two-Body Analyses for a  
8680 kg Load, Three G-12 Parachutes, with  $R_p/M = 7G$

Time (sec)	Altitude (m)		Velocity ( $\frac{m}{s}$ )		Acceleration (G)	
	1-Body	2-Body	1-Body	2-Body	1-Body	2-Body
0	2.00	2.00	15.50	15.50	7.00	7.00
.05	1.31	1.31	12.17	12.17	6.62	6.81
.10	.78	.78	9.00	8.96	6.34	6.23
.15	.41	.41	5.94	6.01	6.15	6.00*
.20	.18	.18	2.96	3.07	6.04	6.00
.25	.11	.10	.02	.19	6.00	6.00

\* Lines slack at  $t = 0.116$  s

## NOMENCLATURE

a	Constant, equal to $G - (R_p/M)$
A	Altitude above sea level, m
$A_f$	Altitude factor
b	Constant, equal to $-G/V_0^2$
c	Integration constant
$C_D$	Drag coefficient
d	Integration constant or nominal parachute diameter, m
D	Parachute drag, N
F	Parachute cluster factor
G, $G_0$	Acceleration of gravity, $9.8 \text{ m/s}^2$ at sea level
h	Length of ground sensing probe or altitude above sea level, m
$H_0$	Load height at probe contact, m
$H_1$	Load height at start of primary rocket thrust, m
$H_2$	Load height at end of primary rocket burn, m
$H_3$	Load height at end of delay period, m
k	Spring constant, kN/m
K	Kurtosis value of a distributed variable
L	Probe length, m
M	Mass of system (load, rockets, parachutes), kg
$M_c$	Parachute mass, kg
$M_i$	Included mass of parachute, kg
$M_L$	Mass of load and retrorockets, kg

$M_{sm}$	System minimum load mass, kg
$n$	Load factor for estimating road loads
$N$	Number of parachutes
$p$	Constant, equal to $c \sqrt{ab}$
$P_o$	Sea level pressure, kPa
$q$	Constant, equal to $\sqrt{ab}$
$R$	Gas constant, m/K
$R_p$	Primary rocket thrust, N
$R_{pn}$	Primary rocket thrust at $T = 288$ K, N
$R_s$	Sustainer rocket thrust, N
$R_{sn}$	Sustainer rocket thrust at $T = 288$ K
$S$	Nominal parachute area, $m^2$ , or skewness of a distributed variable
$t$	Time, s
$t_d$	Delay time, s
$t_i$	Time from either primary burnout to impact, or sustainer rocket ignition to impact, s
$t_p$	Primary rocket burn time, s
$t_r$	Sensor delay and primary thrust buildup time, s
$t_s$	Sustainer rocket burn time, s
$T$	Ambient temperature, K
$T_o$	Characteristic propellant temperature, K, or standard sea level temperature, K
$T_p$	Propellant temperature, K
$V_o$	Load vertical descent velocity, m/s
$V_2$	Load vertical velocity at end of primary rocket burnout, m/s
$V_3$	Load vertical velocity at end of delay period, m/s

$V_h$	Horizontal Velocity due to wind, m/s
$V_i$	Load vertical impact velocity, m/s
$W$	Weight of load, lb
$x$	Distance of load above ground, m
$x_c$	Distance above ground of center of mass of parachutes, m
$x_L$	Distance above ground of center of mass of load and retrorockets, m
$\Delta x$	Change in position difference of parachutes and load, m
$\Delta x_o$	Steady descent value of $\Delta x$ , equal to $\Delta x_r + \Delta x_s$ , m
$\Delta x_r$	Riser line stretch at steady descent, m
$\Delta x_s$	Suspension line stretch at steady descent, m
$z$	Position difference between parachutes and load at steady descent, m, or time derivative of $x$ , m/s
$\alpha$	Terrain slope angle, degrees
$\theta$	System attitude angle, degrees
$\sigma$	Standard deviation
$\rho$	Air density, kg/m <sup>3</sup>
$\rho_o$	Air density at sea level, kg/m <sup>3</sup>
$\tau$	Total suspension line tension, N